Operational use of Timepix-based Radiation Environment Monitors on ISS

Tom Campbell-Ricketts,
Leidos Inc, NASA Space Radiation Analysis Group

25th WRMISS, Mons, Belgium,
September 2022

Radiation Environment Monitors

Team:

Nic Stoffle, Stuart George, Andrew Castro, Tom Campbell-Ricketts, Daniel Turecek (Prague)

Technology demo from 2012 to 2019

7 units operational from February 10th 2019

- Timepix, hybrid detector
- Minipix readout
- 500 µm Si sensor
- 256 x 256 pixels
- pixel pitch = 55 µm
- time-over-threshold energy resolution (5 keV threshold)
- frame length from ms to ∞
- adaptive shutter algorithm
- connected to SSCs

Overview

(1) Routine data products

(2) Special topics

- (2.1) SAA dose rate variability
- (2.2) Single-layer telescope

REM2 Science Report - 07/24/22 - 07/31/22 (2022 GMT 205 - 2022 GMT 212)

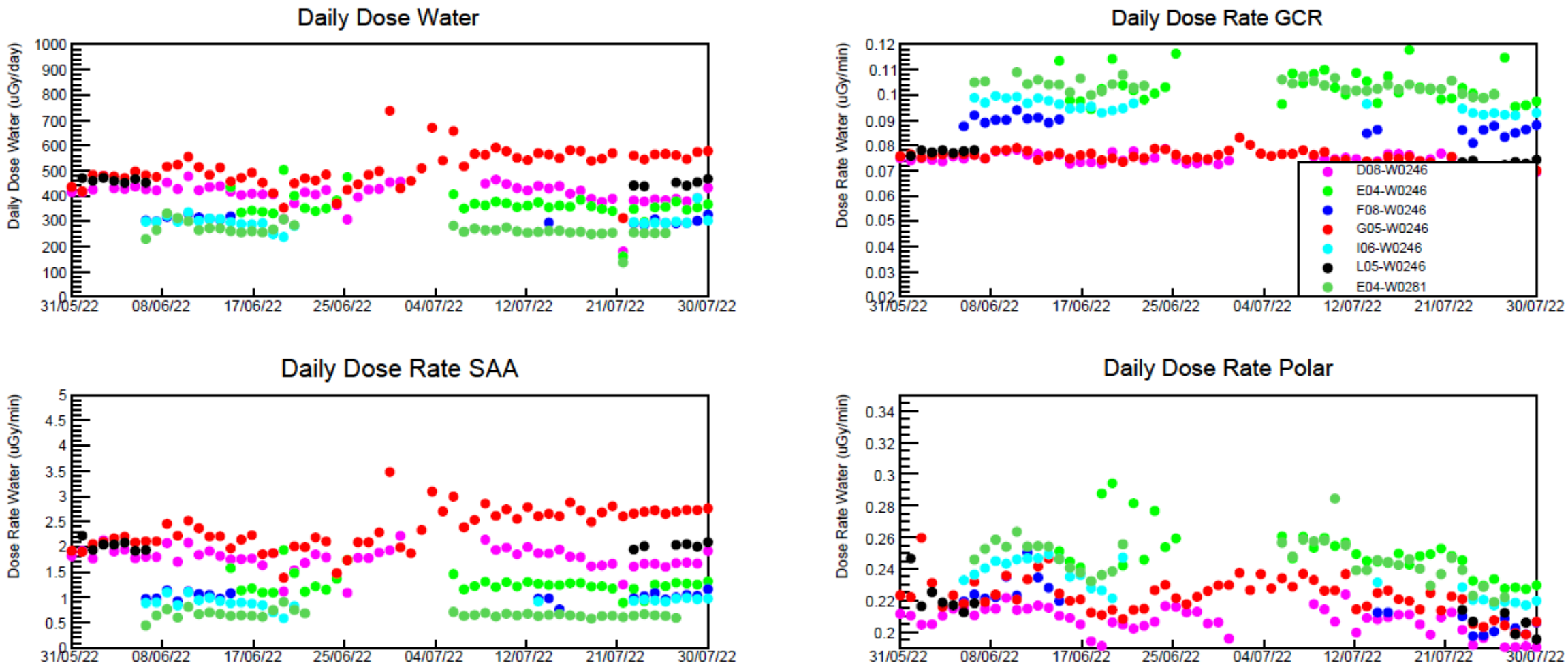

Figure 1: REM2 Daily absorbed dose rates in water for last 60 days. SAA : McIlwain L < 3, B < 23000 nT, Polar : L > 3, GCR : not SAA (includes Polar).

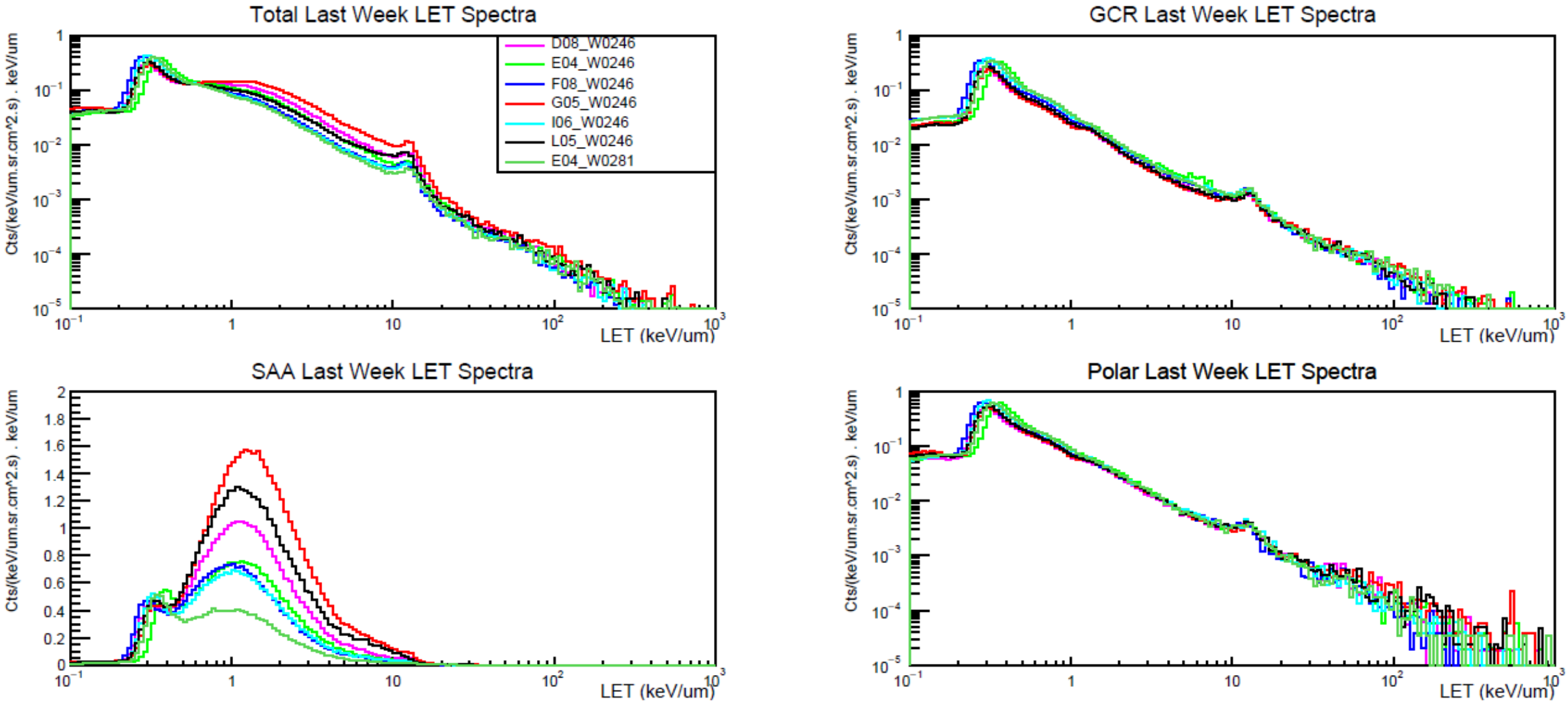

Figure 2: REM2 LET Spectra in silicon over last week (flux * LET to preserve visual area with log(x) scale).

Detector Health Metrics

Detector	Location	Livetime %	Dead Px	Delta	Bright Px	Delta	Noisy Frame	High Px
F08-W0246	CUPOLA	95.9	1	0	0	0	54.1	0.1
L05-W0246	NOD1P4O3	77.4	16	0	0	0	0.5	0.0
D08-W0246	NOD30A2	98.9	0	0	0	0	78.7	0.0
E04-W0281	LAB1PD3	55.4	2	0	0	0	18.0	0.0
E04-W0246	JPM1FD4	98.4	38	1	1	0	66.7	0.4
I06-W0246	LAB1O5A2	99.1	4	0	0	0	48.9	0.1
G05-W0246	COL1A3	99.6	2	0	0	0	10.9	0.3

Table 2: Table of detector health metrics. Livetime is the fraction of time the detector was on for the week. Bright pixels are pixels that count consistently high, dead pixels count consistently low or are masked. Bright and dead pixels show the highest daily number for the week. Delta shows the change in this quantity from the last week. Noisy frames are average per day. High px gives the daily average of pixel counts over 4 MeV for the week.

- Detectors experience downtime due to issues with the laptops
- Doesn’t mean that the dose was zero during that period!
- We still have a duty to provide best possible estimate of the radiation period exposure during downtime.
- Use a backfilling procedure to estimate what the most likely dose was during downtime
- Estimate based on recent data taken at similar lat/lon/altitude coordinates

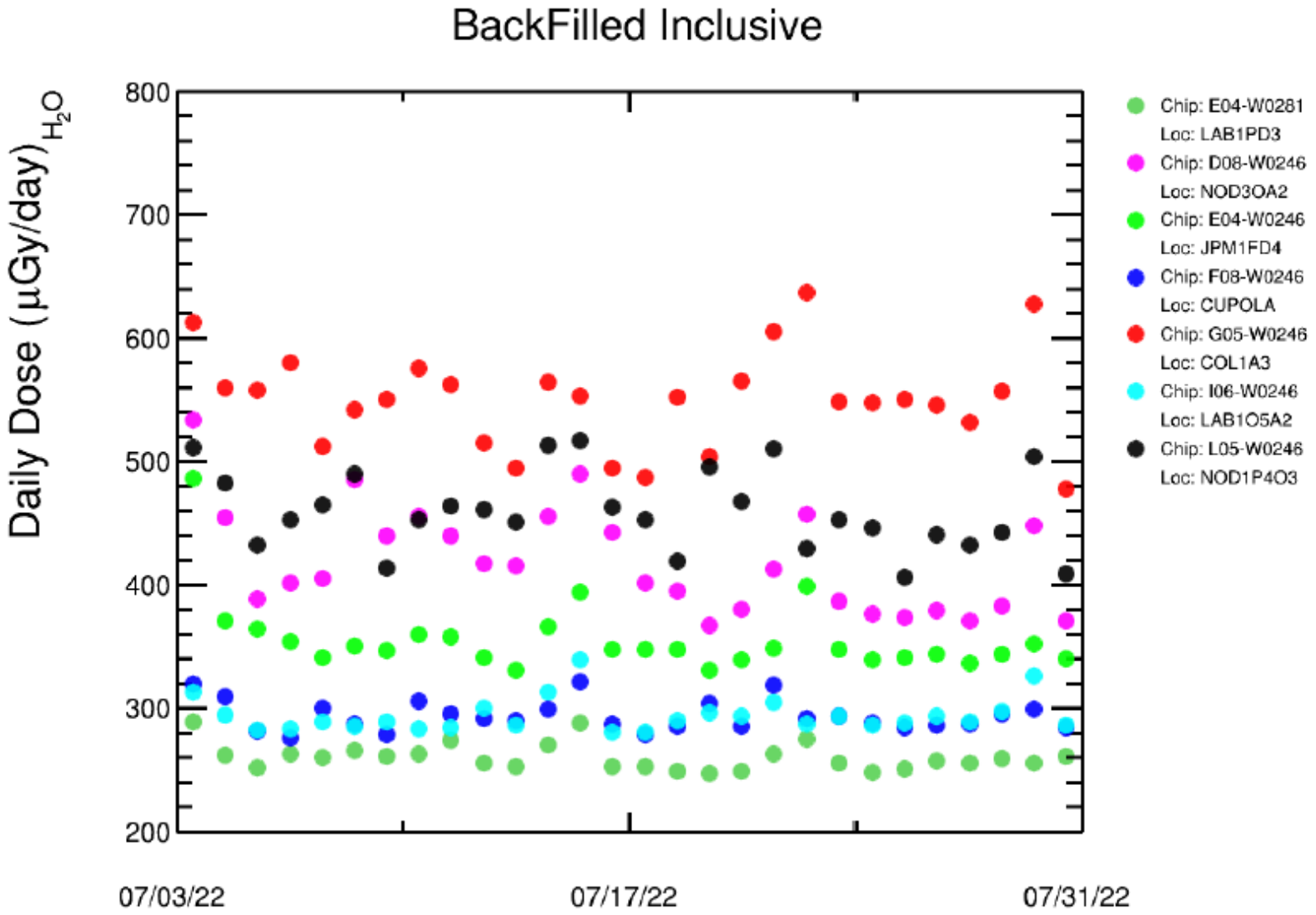

Reduced Data Format

- Daily data files (pixel cluster data) reduced down to a set of per-minute dose rates and LET flux spectra
- Allows fast access to the data products that matter most
- Eliminates need for expertise in Timepix & the REM data acquisition protocols
  - principal data set given to people outside REM analysis group in SRAG
- rdf files generated daily and archived all the way back to the detectors coming online in 2019
- Flux rates are corrected for angle of incidence
  - for each incident particle, count is scaled by 1/projected area, obtained from measured azimuth and polar angle

Reduced Data Format

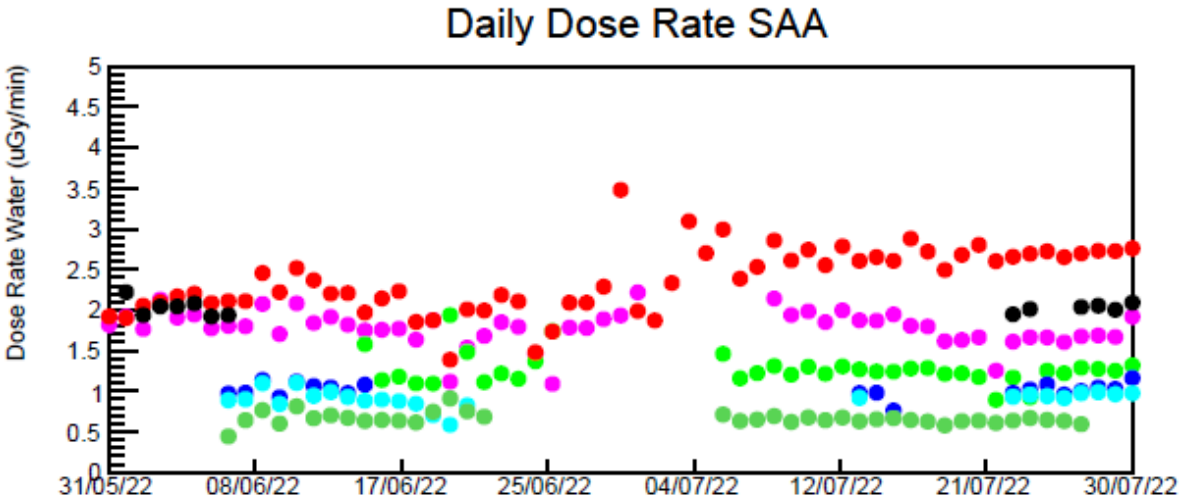

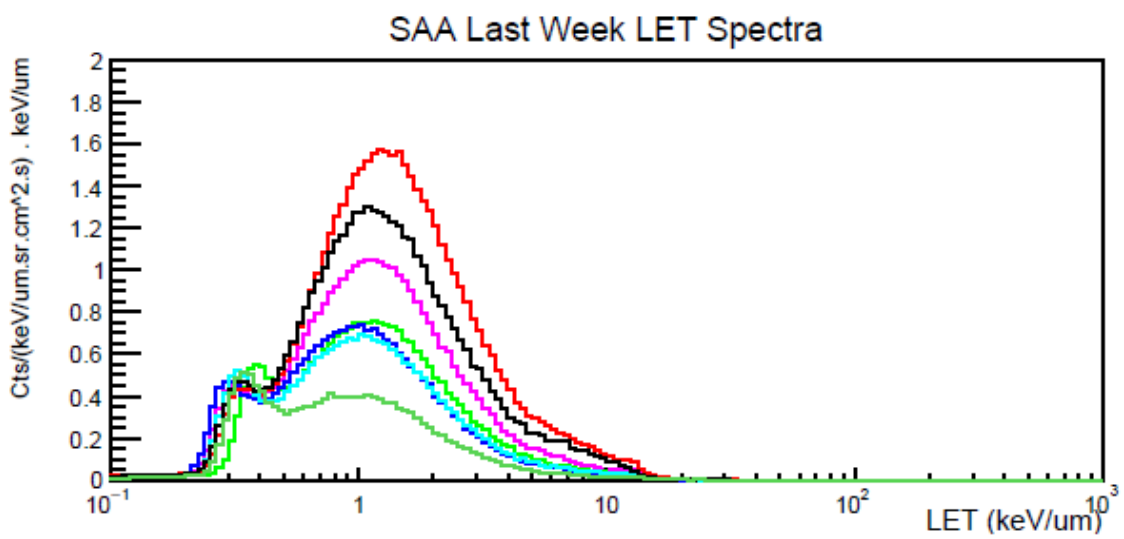

Detector dose rates & integrated fluxes in SAA show the same ordering following angular flux correction.

Without this correction, detector ranking by dose rate is completely different to ranking by particle flux.

SAA variability

- Large differences between detectors when we look at dose & fluxes in SAA
  - Different detector orientation?
  - Different shielding environment?

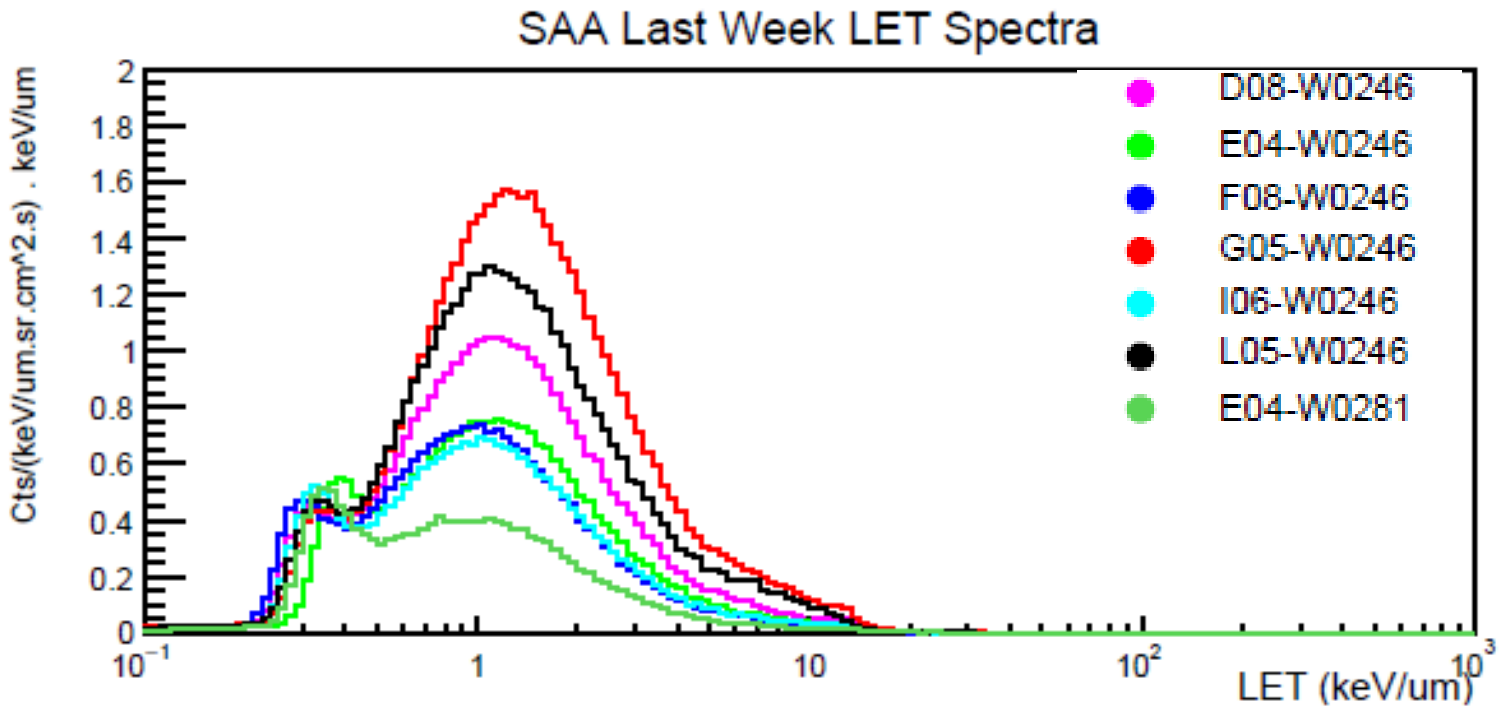

SAA variability

- Large differences between detectors when we look at dose & fluxes in SAA
  - Different detector orientation?
  - Different shielding environment?
- East-West asymmetry for trapped radiation is known, and results from gyration of particles around field lines
  - Looking North, protons gyrate anticlockwise, meaning that protons arriving from the West are in higher orbits than protons from the East
  - Lower orbits pass through thicker atmosphere, though, therefore fewer particles

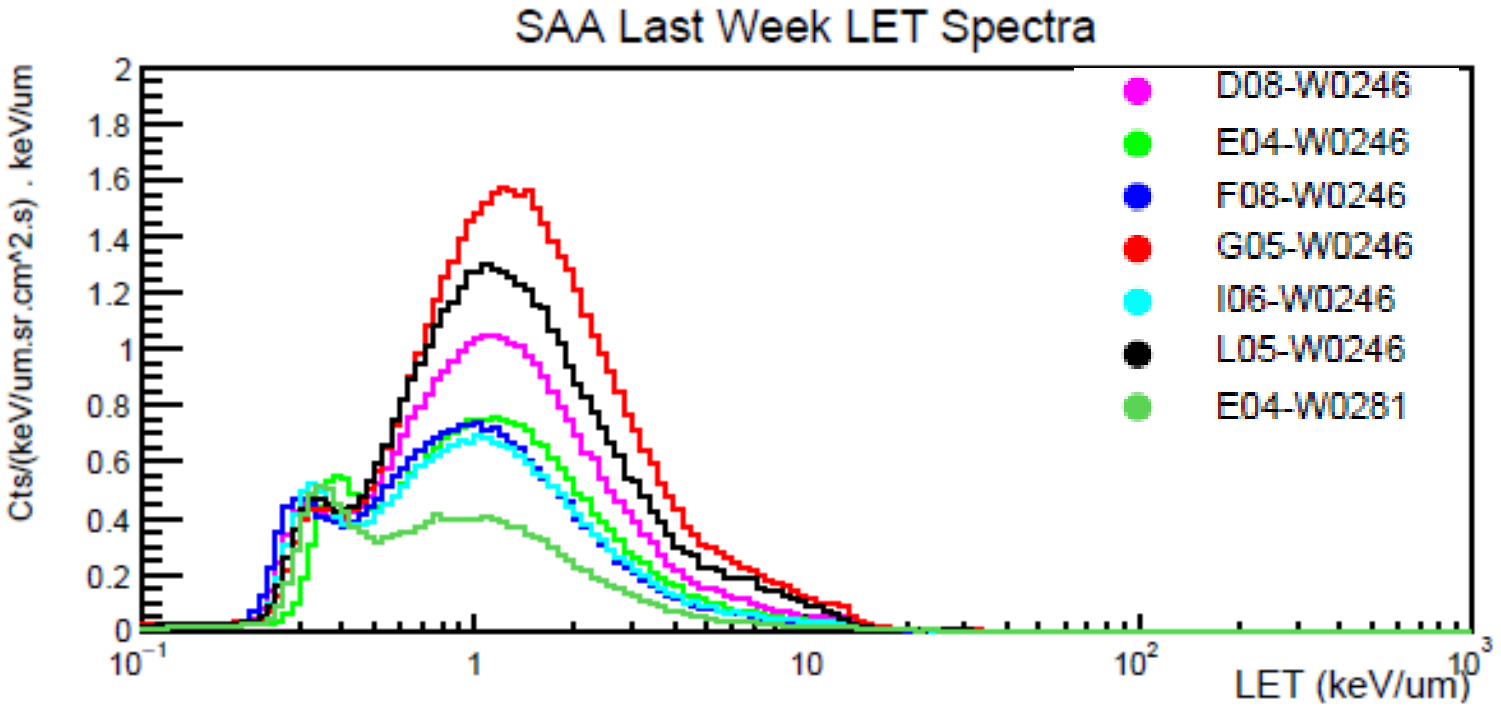

East-West effect

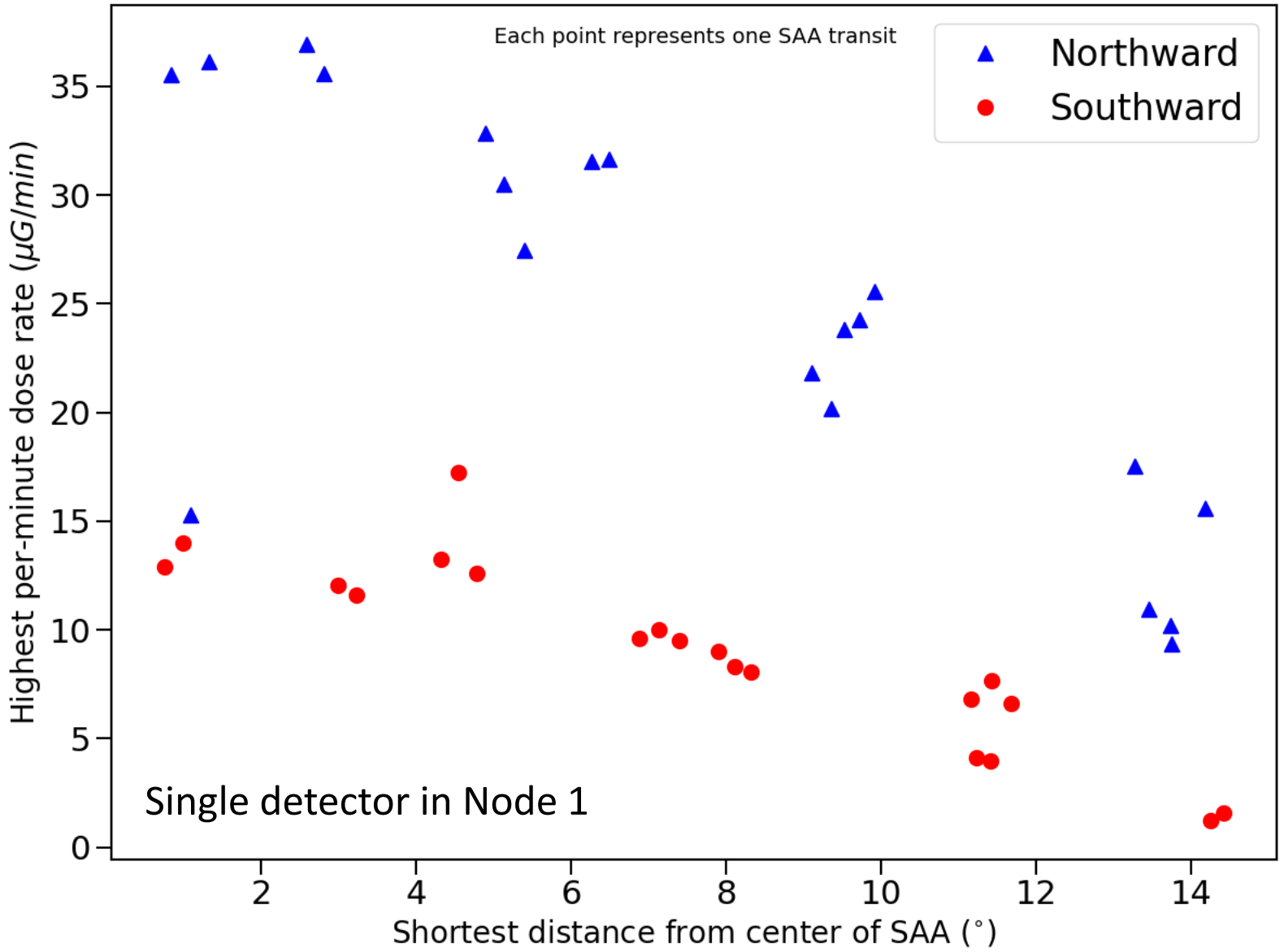

East-West effect

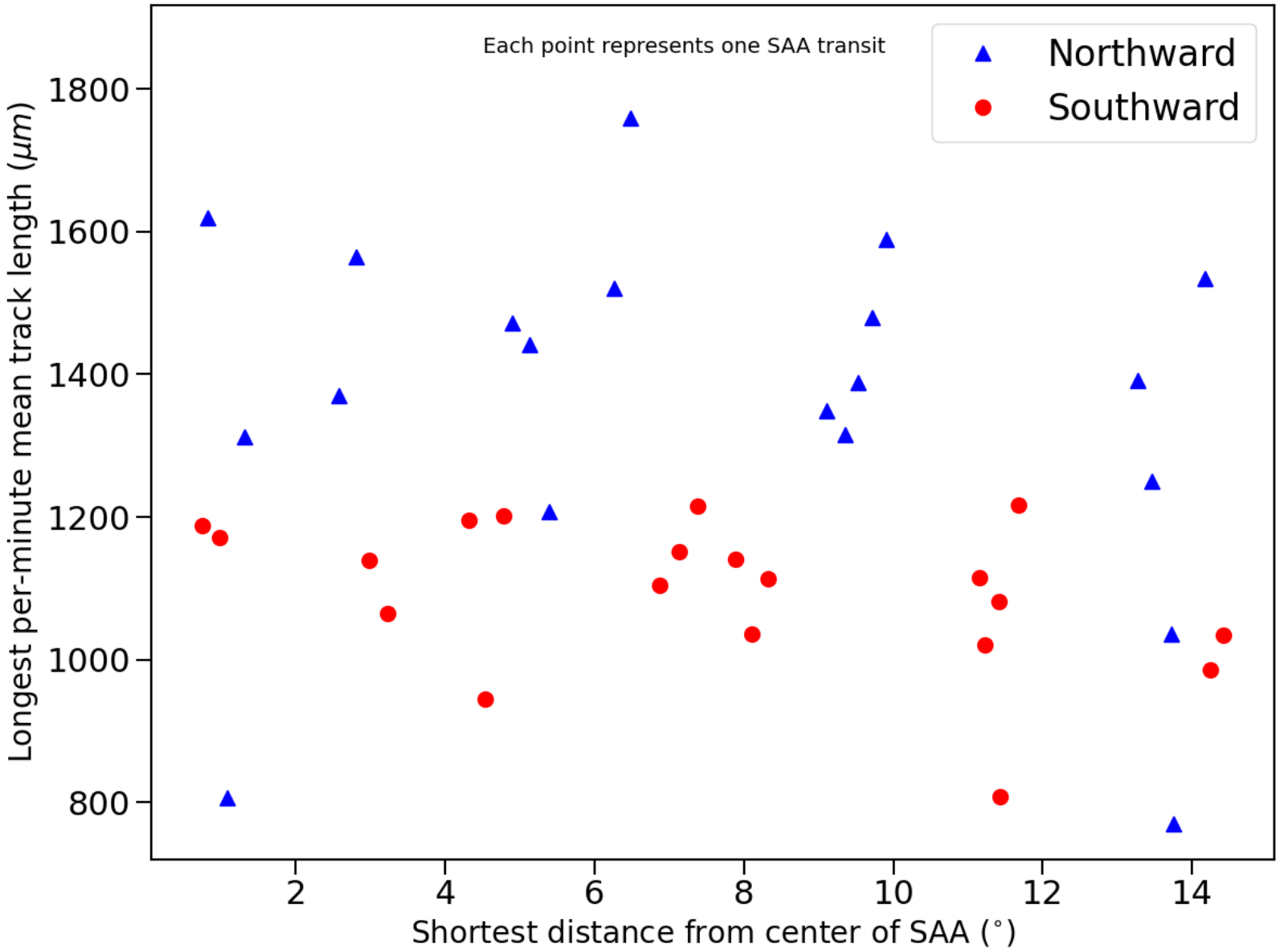

East-West effect

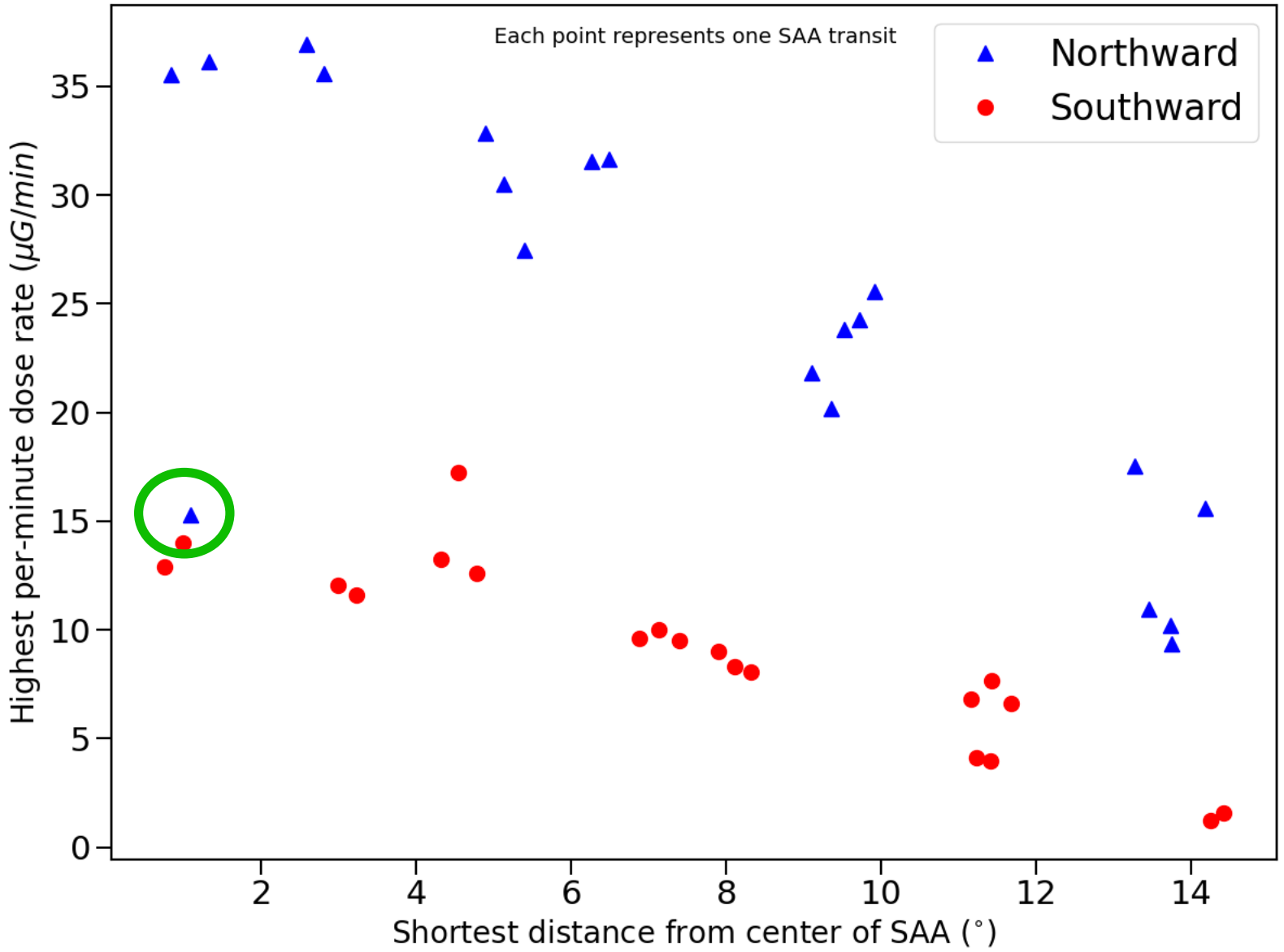

East-West effect

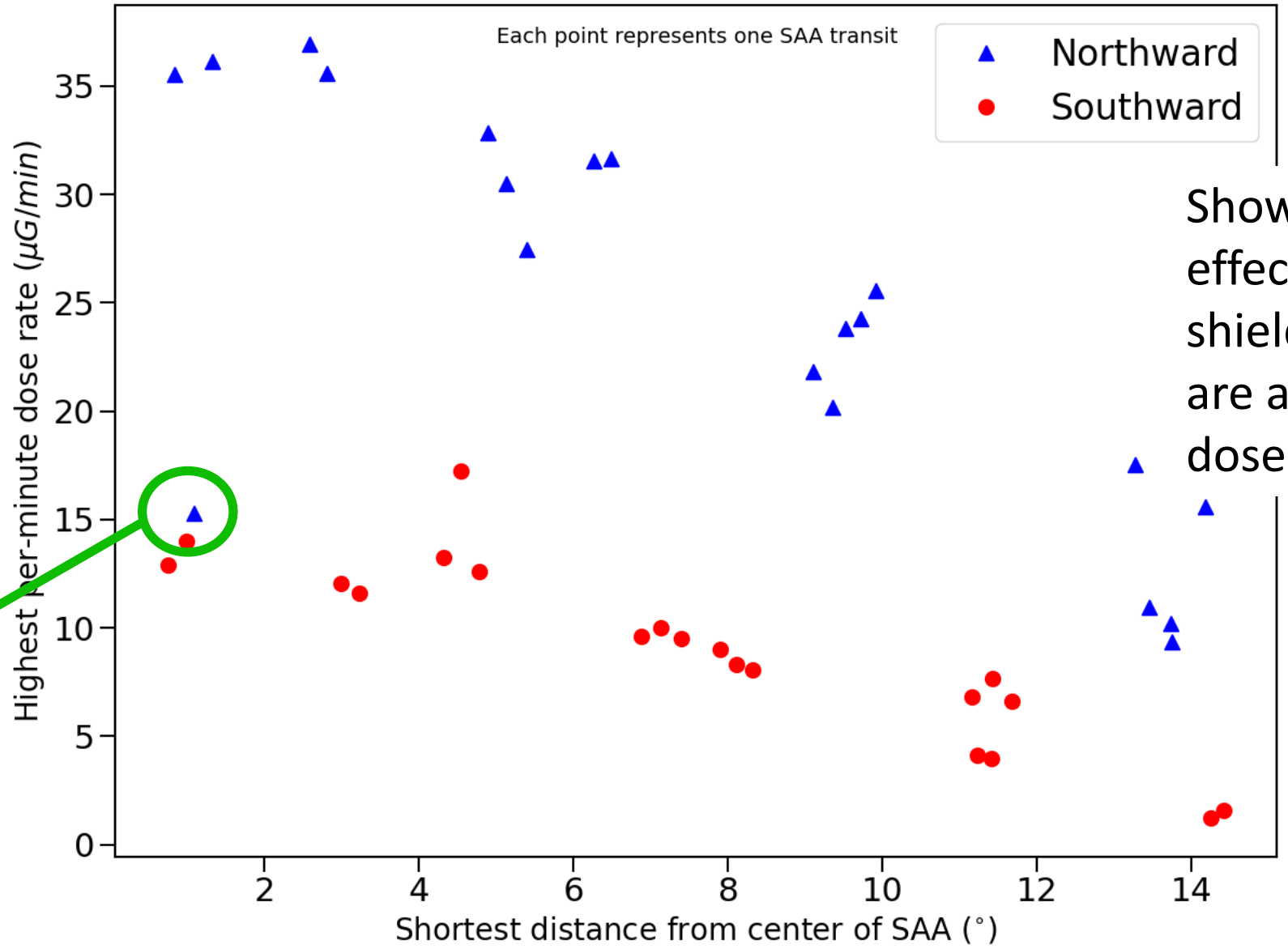

Brief attitude adjustment on 7/23/2020: rotated 180° around z-axis

Shows that East-West effect, coupled with shielding conditions are a major cause of dose variability in SAA

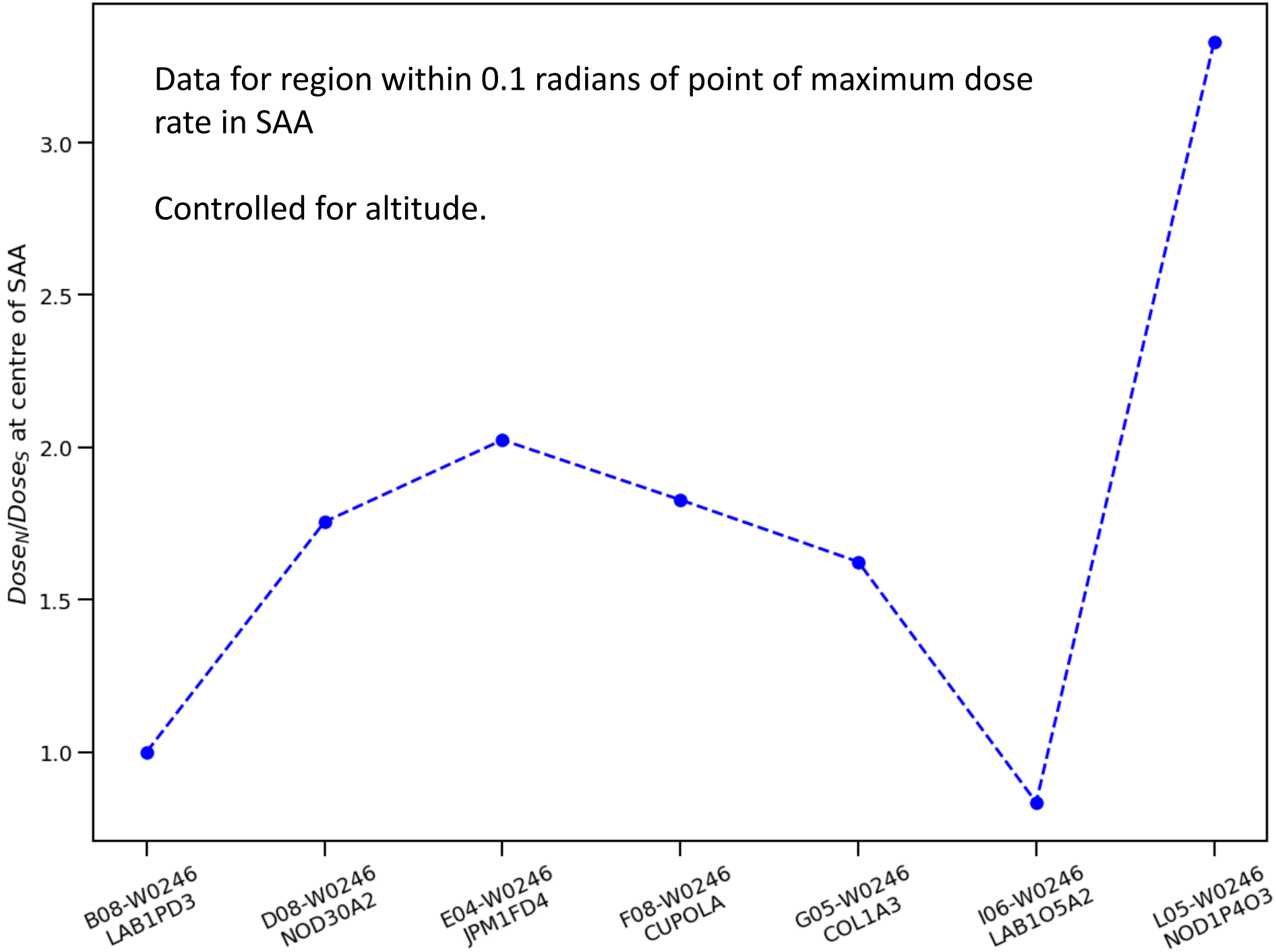
Data for region within 0.1 radians of point of maximum dose rate in SAA
Controlled for altitude.
$Dose_N/Dose_S$ at centre of SAA
3.0
2.5
2.0
1.5
1.0
B08-W0246 LAB1PD3
D08-W0246 NOD30A2
E04-W0246 JPM1FD4
F08-W0246 CUPOLA
G05-W0246 COL1A3
I06-W0246 LAB1O5A2
L05-W0246 NOD1P4O3

Single-layer telescope

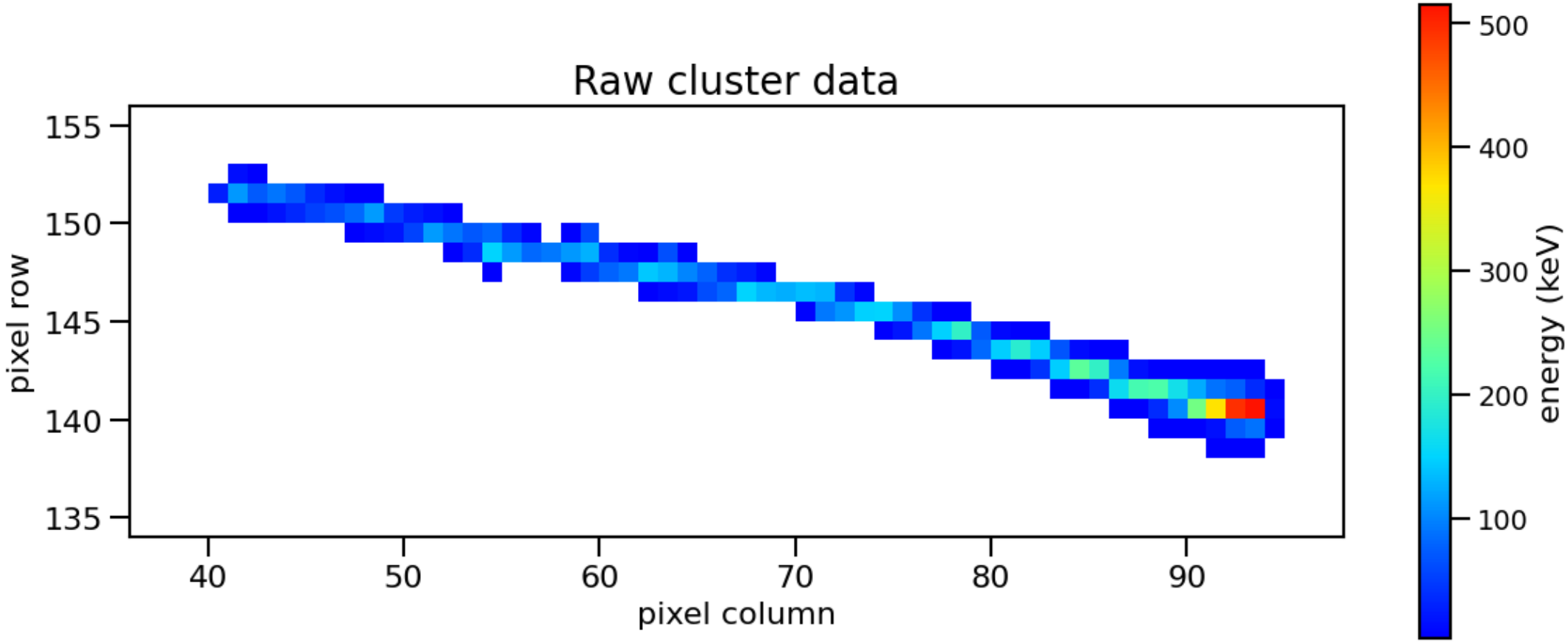

Single-layer telescope

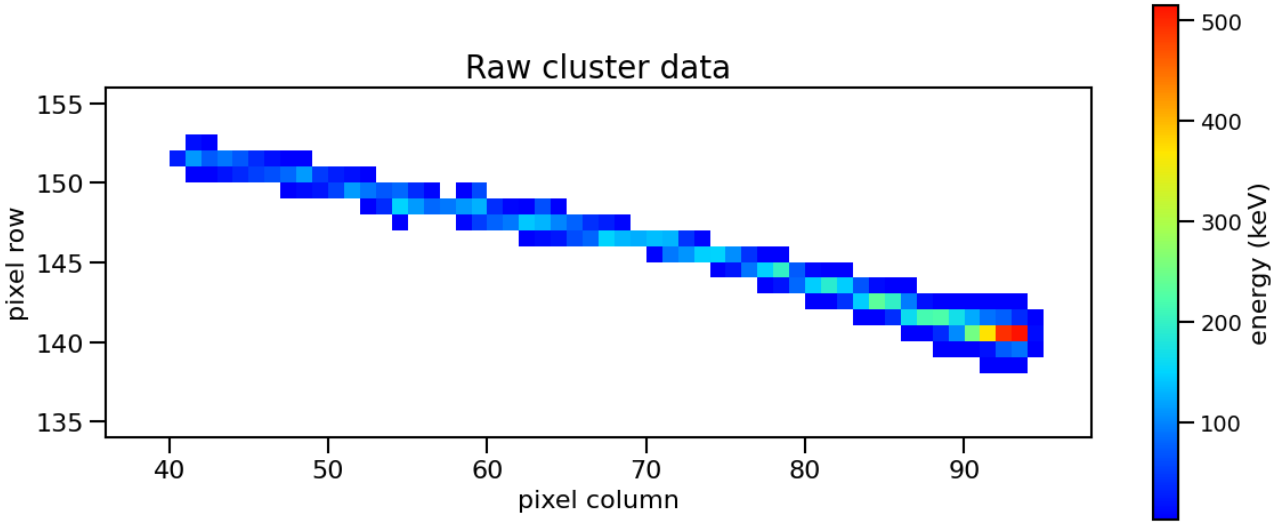

Image analysis gives track length, which coupled with deposited energy gives dE/dx

Single-layer telescope

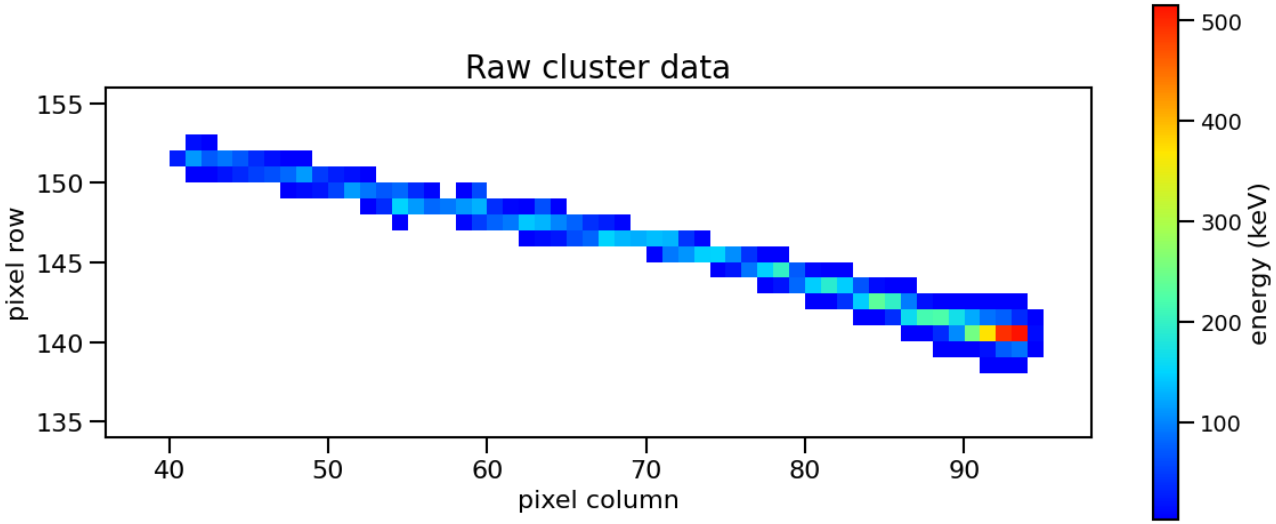

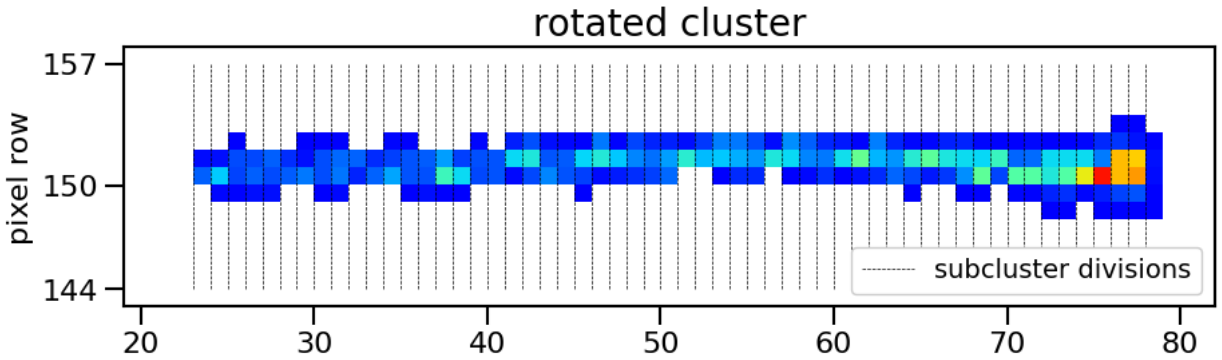

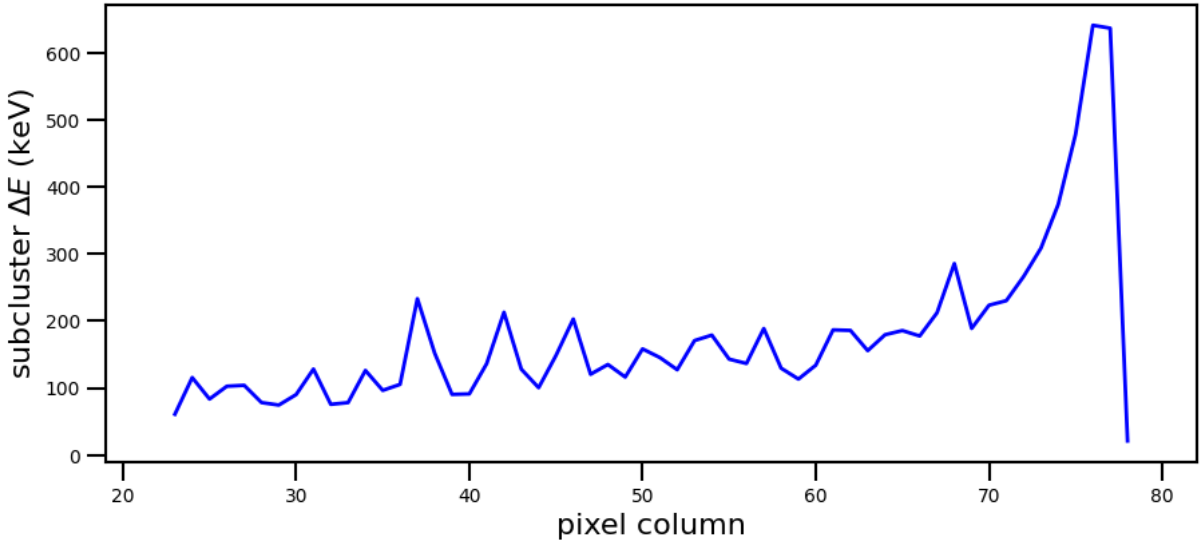

Pixel data becomes the equivalent of a particle telescope with a stack of >50 detector layers

Single-layer telescope

'Kinetic energy reconstruction with a single layer particle telescope,' Kroupa *et al*., Applied Physics Letters 112, 134103 (2018)

(1) Energy ID

$$P(E_j \mid \Delta E_1, \ldots, \Delta E_n, \Delta x) \propto P(E_j) \times \prod_{i=2}^{n-1} P(\Delta E_i \mid E_j, \Delta x)$$

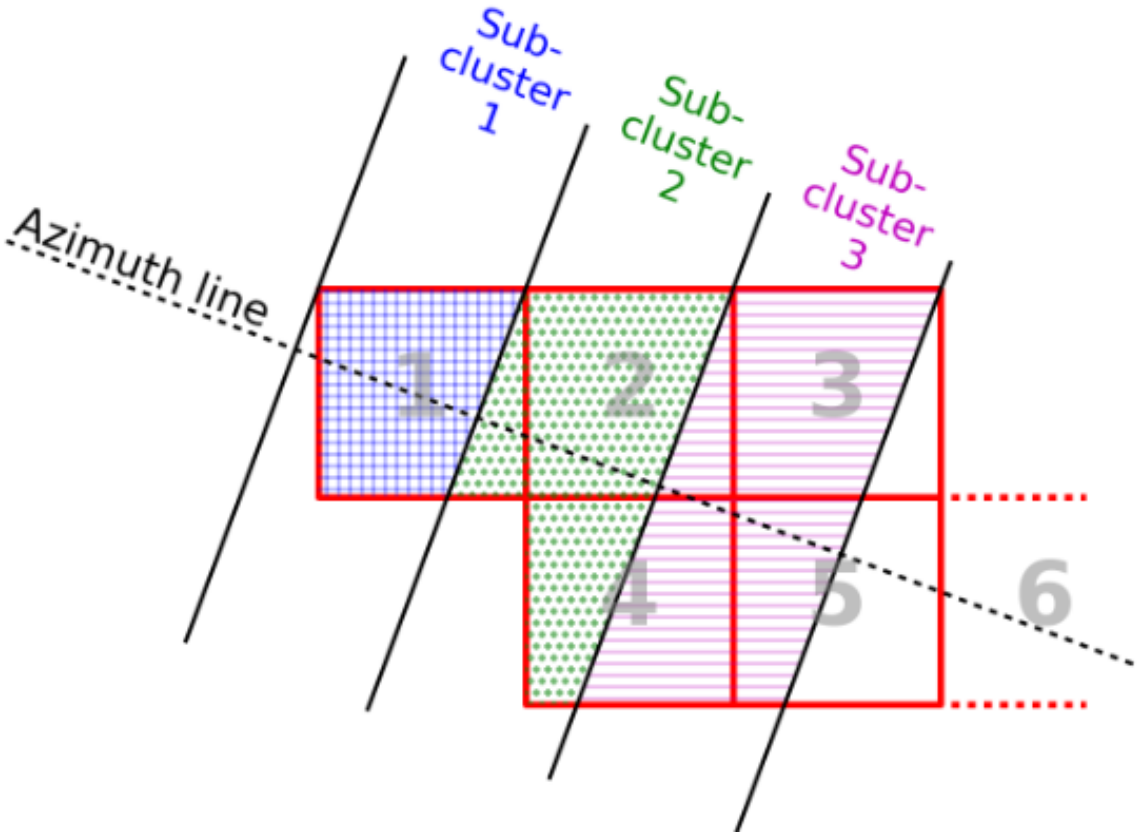

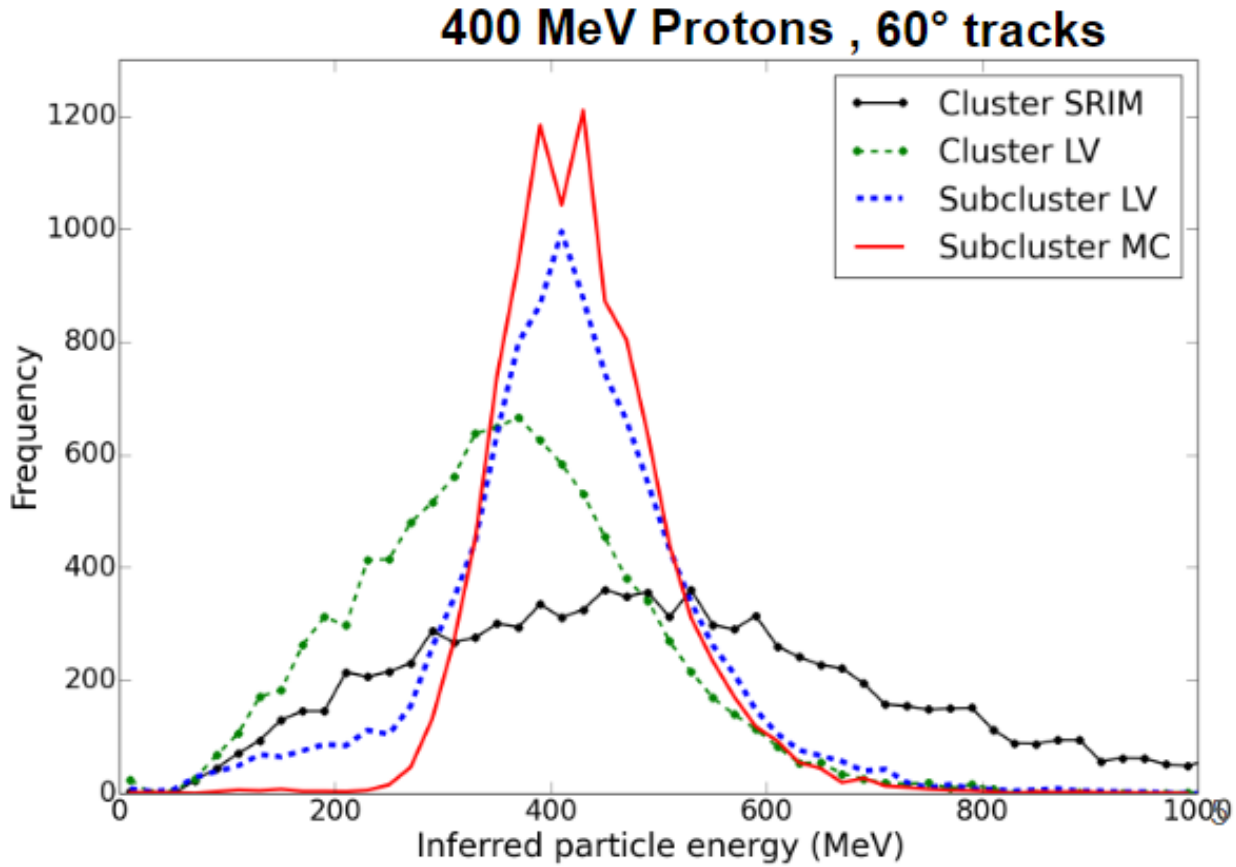

Single-layer telescope

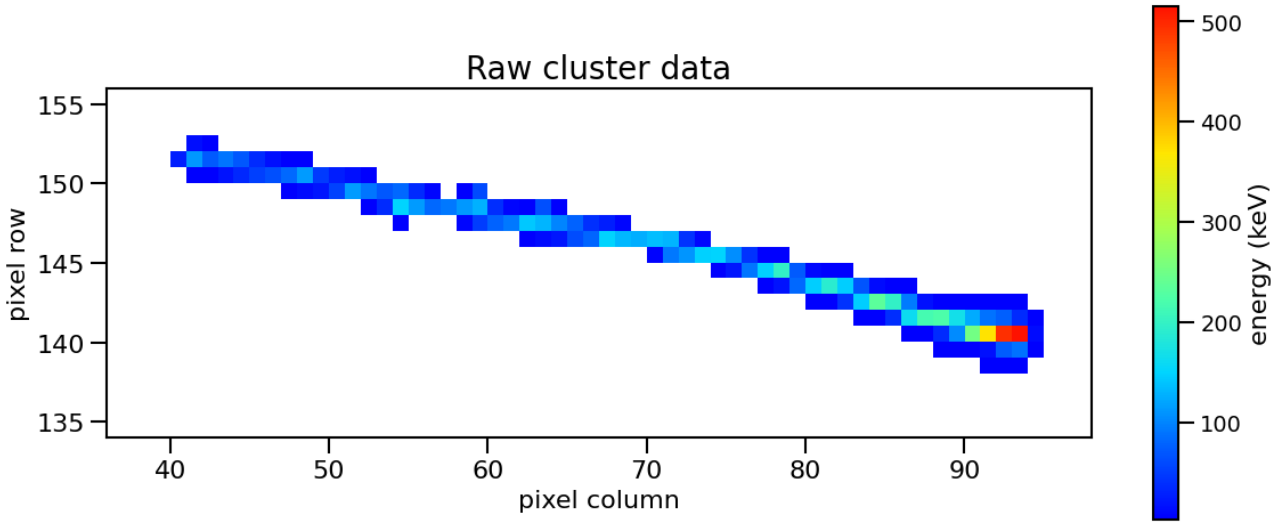

Δx is constant for each subcluster in each track (500 µm in this case)

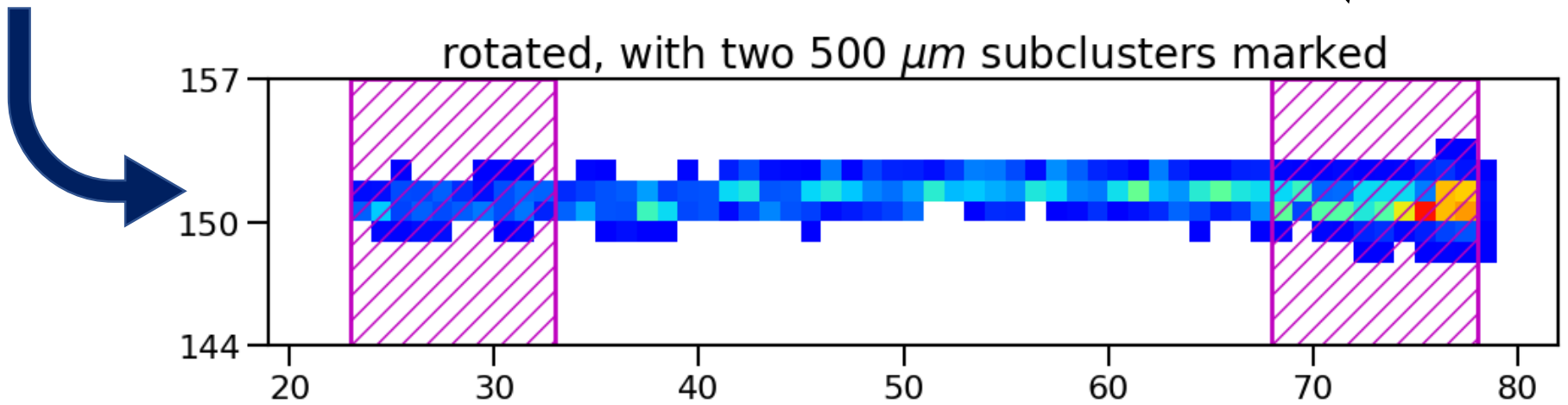

Single-layer telescope

(2) ΔE vs ΔE plots

‘Light ion isotope identification in space using pixel detector based single layer telescope,’ Kroupa *et al*., Applied Physics Letters 113, 174101, (2018)

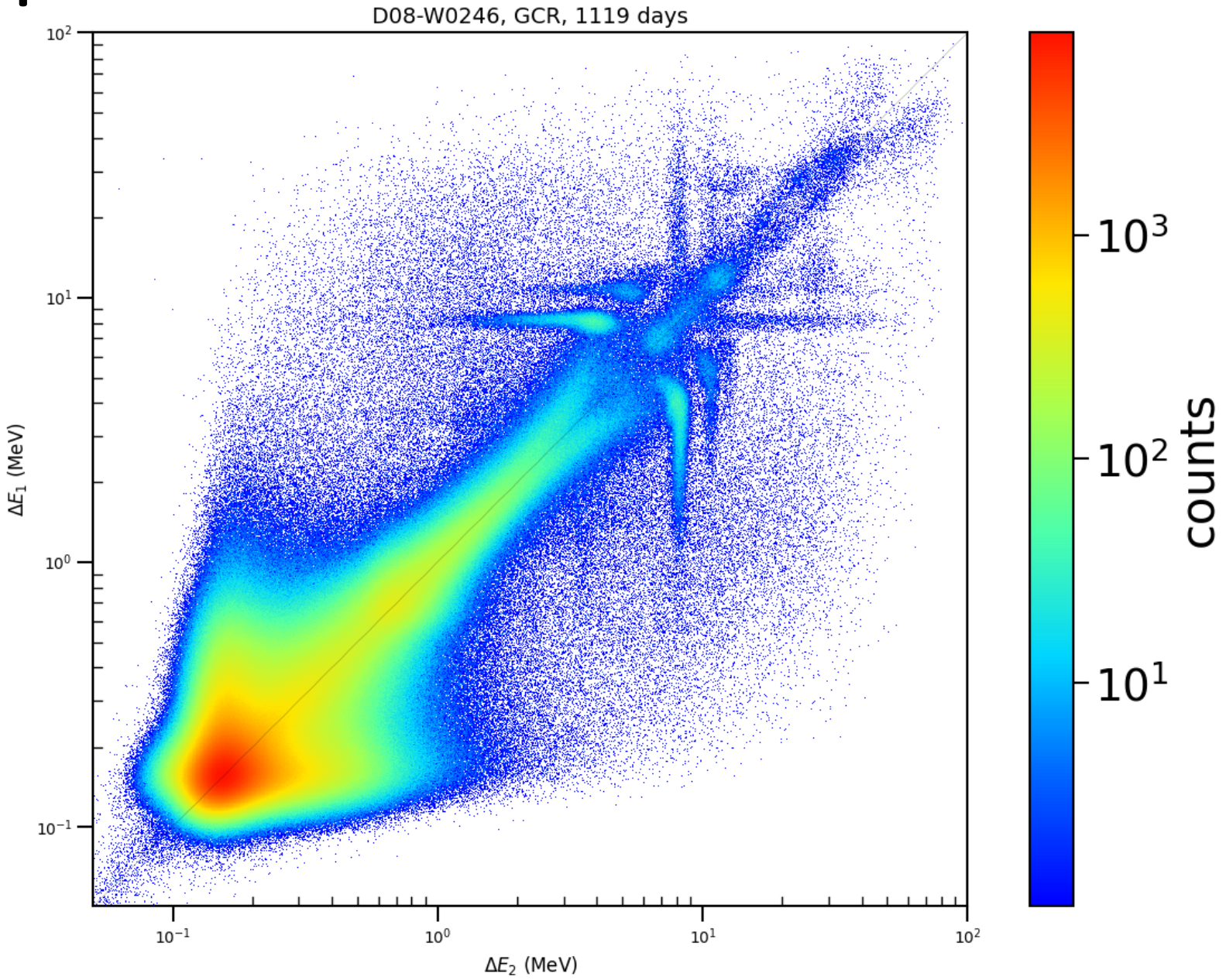

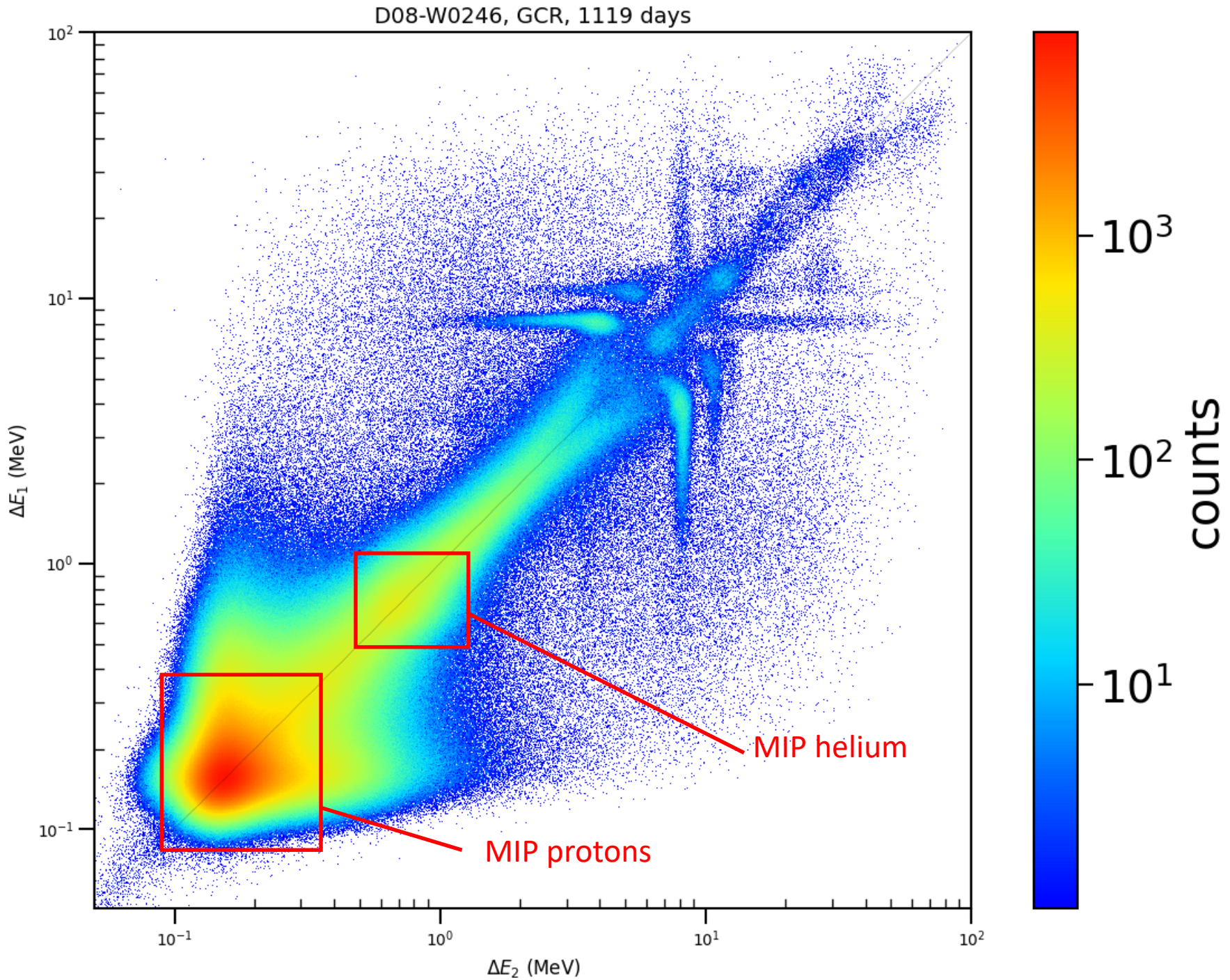
D08-W0246, GCR, 1119 days
10^2
10^1
10^0
10^{-1}
ΔE_1 (MeV)
10^{-1}
10^0
10^1
10^2
ΔE_2 (MeV)
MIP helium
MIP protons
10^3
10^2
10^1
counts

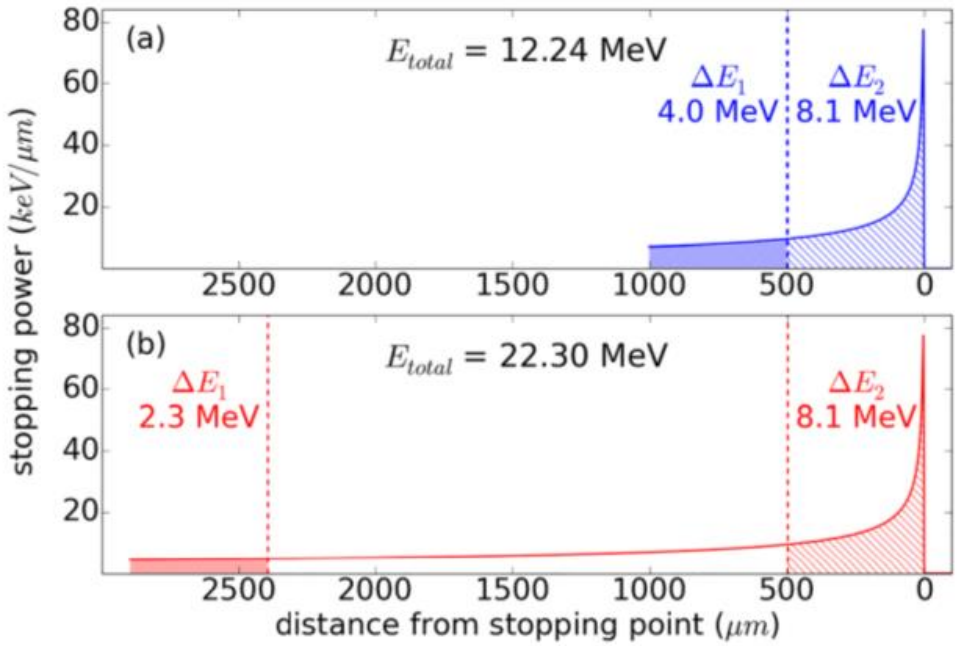

FIG. 1. Theoretical proton stopping curves in silicon for two different initial energies. The curves were calculated using the Bethe formula.[17] The regions corresponding to 500 μm at either end of the track are marked with dashed lines.

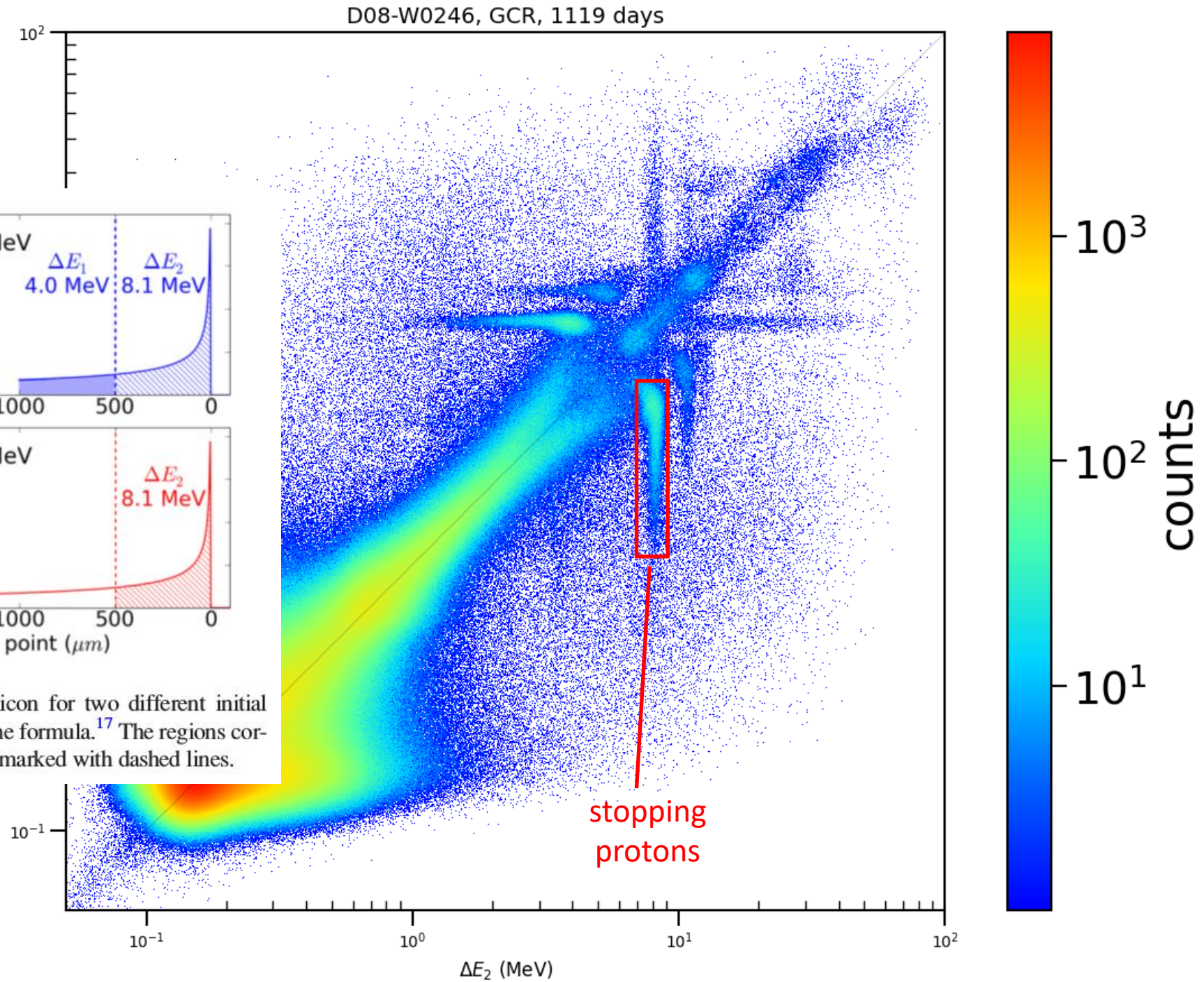

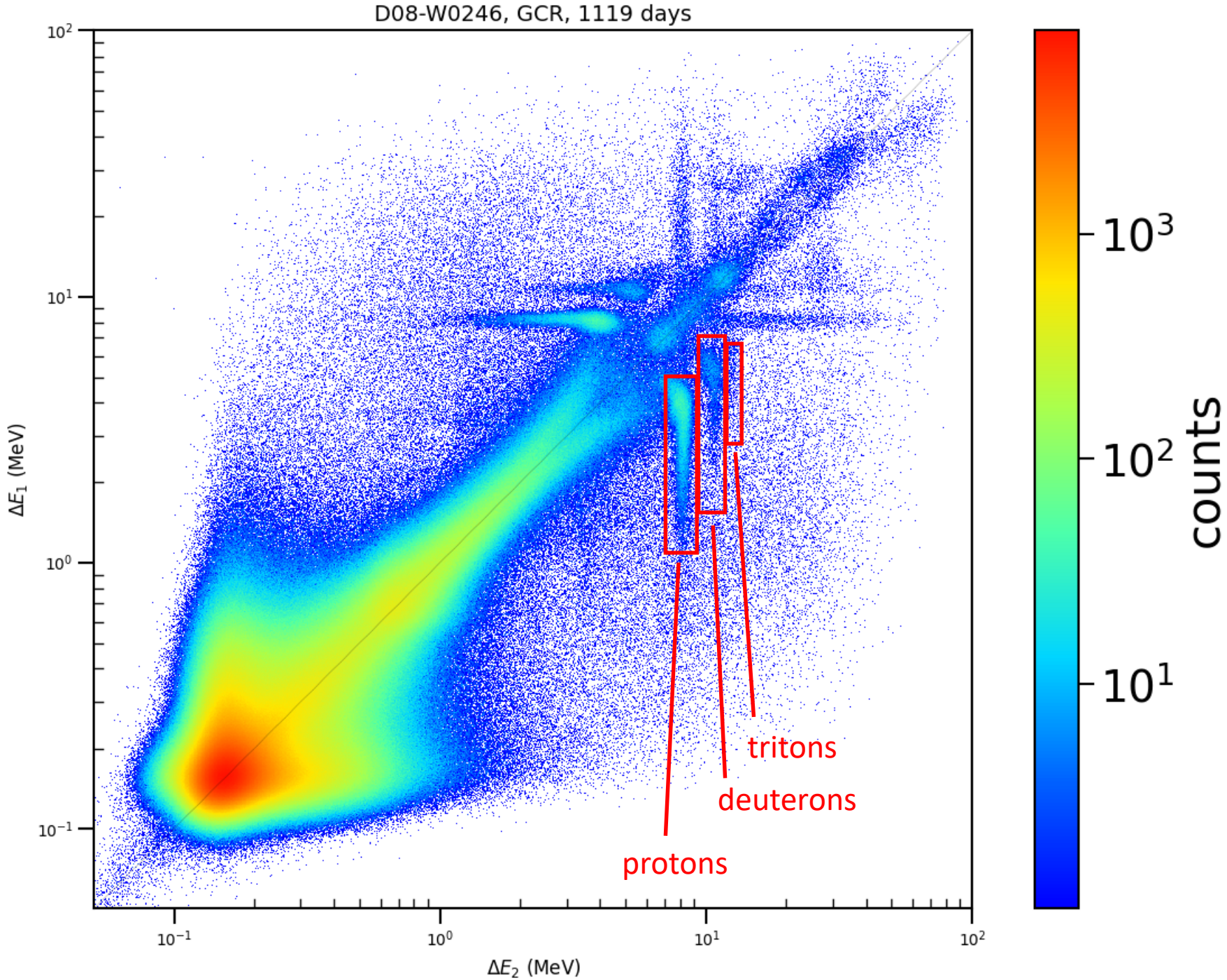
D08-W0246, GCR, 1119 days
10^2
10^1
10^0
10^{-1}
ΔE_1 (MeV)
10^{-1}
10^0
10^1
10^2
ΔE_2 (MeV)
protons
deuterons
tritons
10^3
10^2
10^1
counts

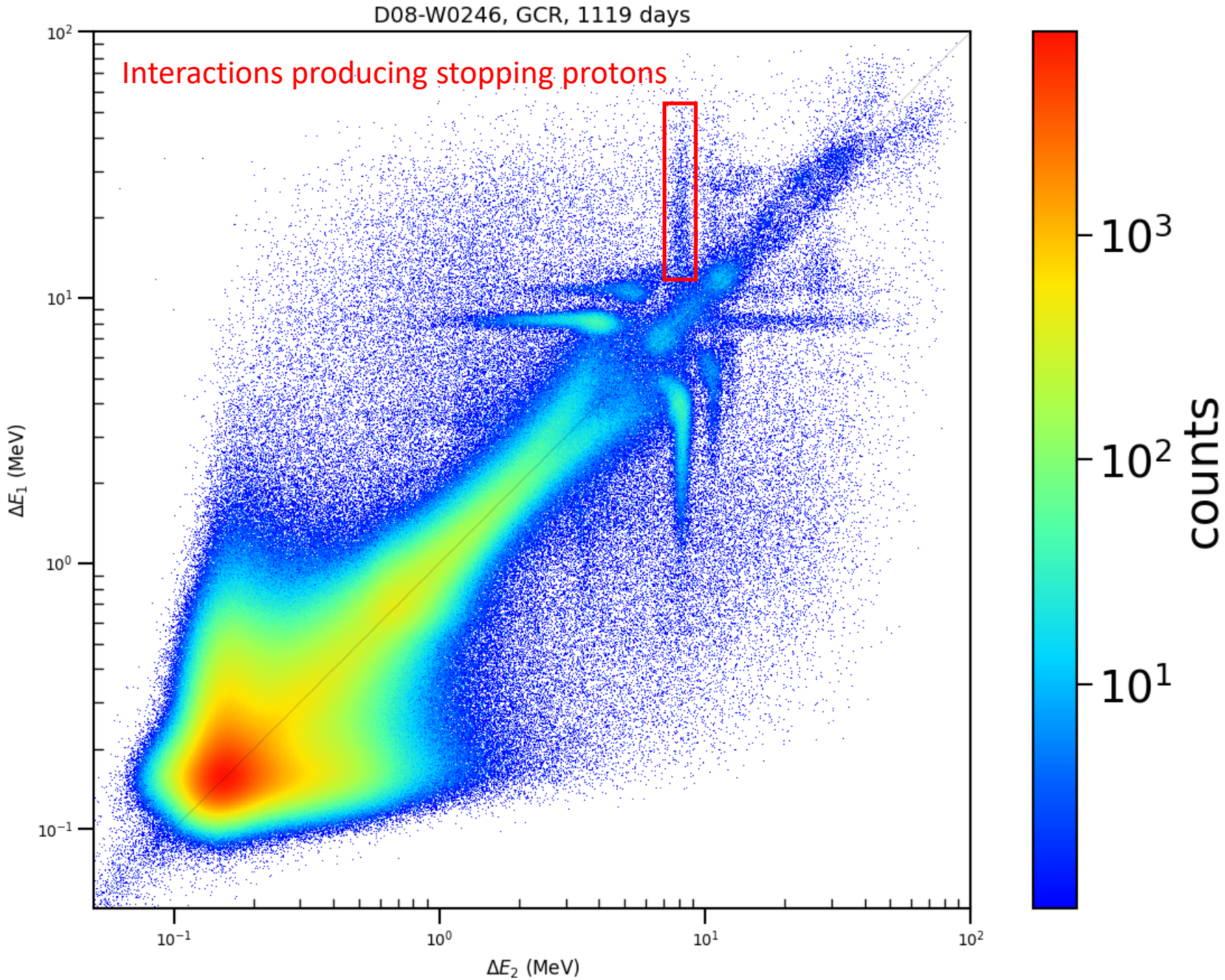
D08-W0246, GCR, 1119 days
Interactions producing stopping protons
10^2
10^1
10^0
10^{-1}
ΔE_1 (MeV)
10^{-1}
10^0
10^1
10^2
ΔE_2 (MeV)
10^3
10^2
10^1
counts

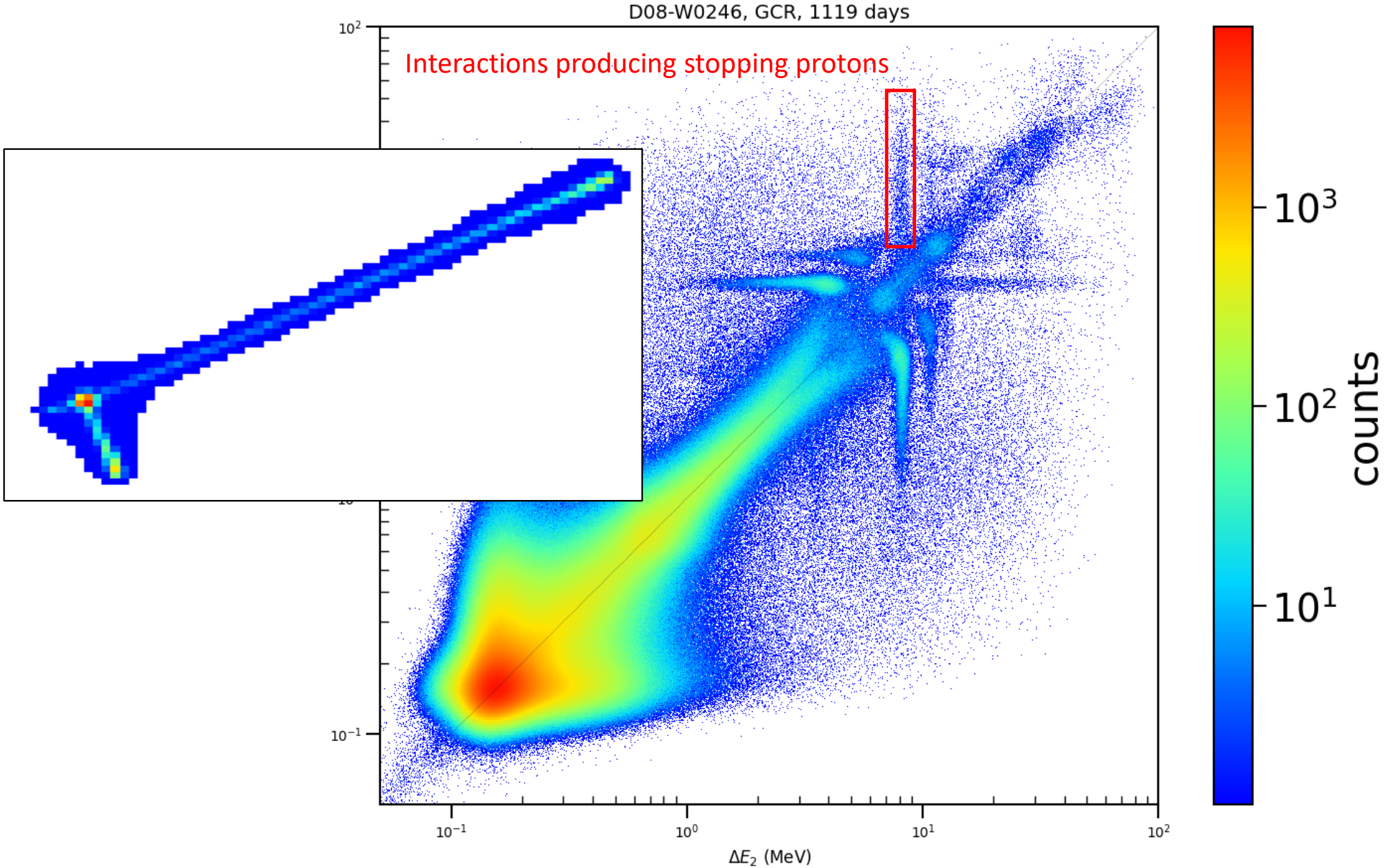
D08-W0246, GCR, 1119 days
Interactions producing stopping protons
10^2
10^{-1}
10^{-1}
10^0
10^1
10^2
ΔE_2 (MeV)
10^3
10^2
10^1
counts

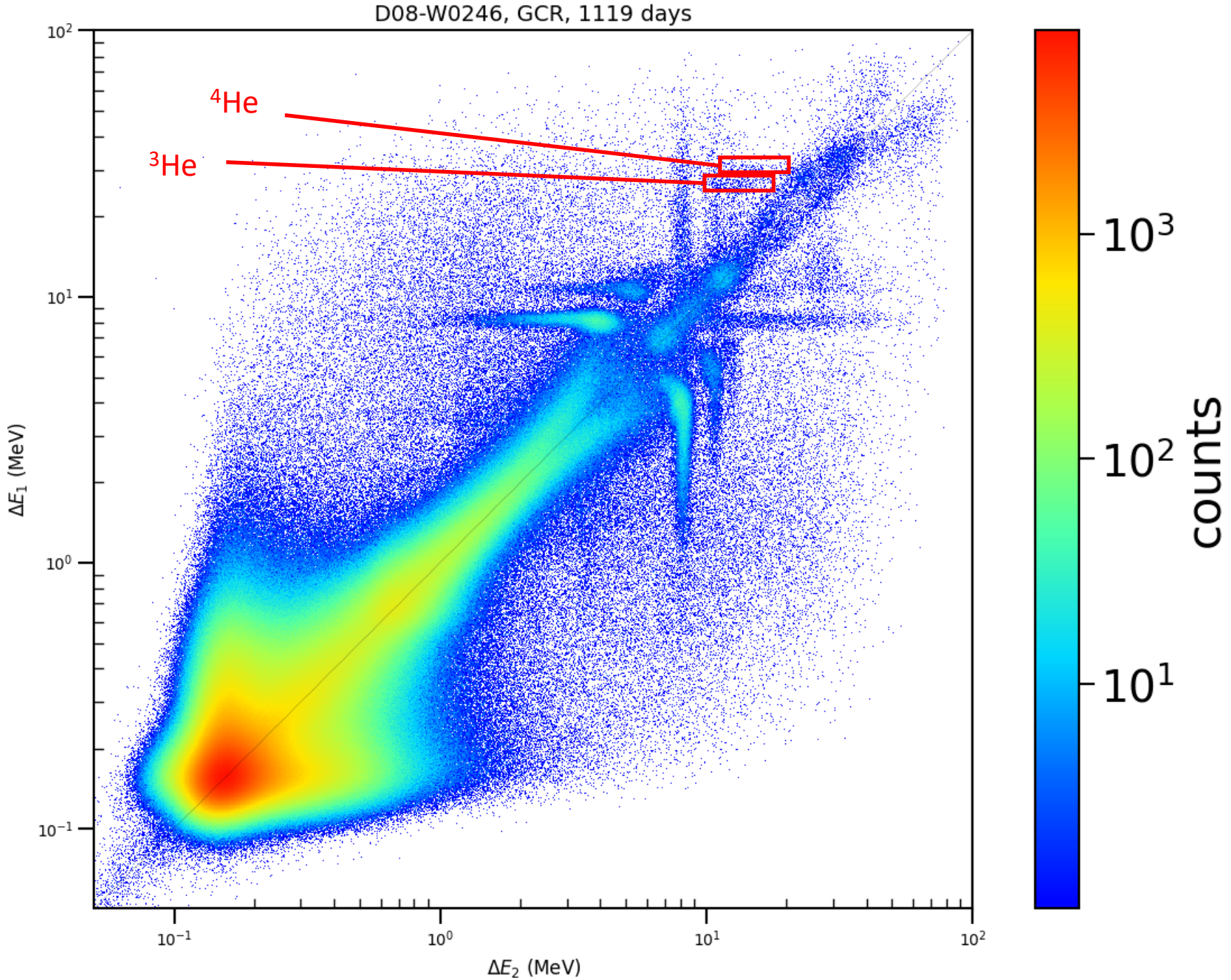
D08-W0246, GCR, 1119 days
^{4}He
^{3}He
10^2
10^1
10^0
10^{-1}
ΔE_1 (MeV)
10^{-1}
10^0
10^1
10^2
ΔE_2 (MeV)
10^3
10^2
10^1
counts

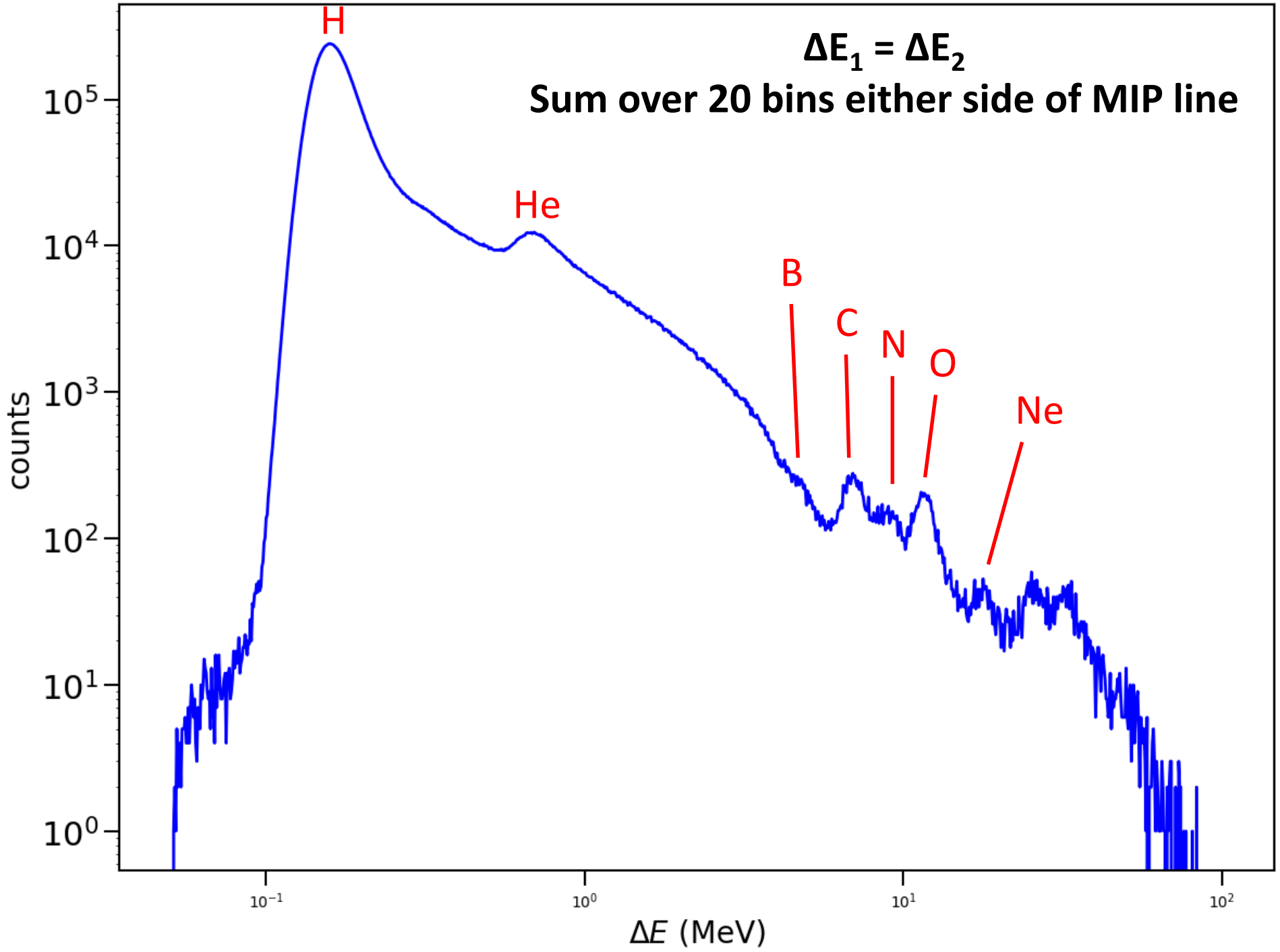
$\Delta E_1 = \Delta E_2$
Sum over 20 bins either side of MIP line
H
He
B
C
N
O
Ne
counts
10^5
10^4
10^3
10^2
10^1
10^0
10^{-1}
10^0
10^1
10^2
ΔE (MeV)

Counts above diagonal added to corresponding location below diagonal for higher SNR.

Polygon marks region of interest for analysis of stopping hydrogen.

Integrate over each vertical strip in ROI to give a 1D spectrum (next slide).

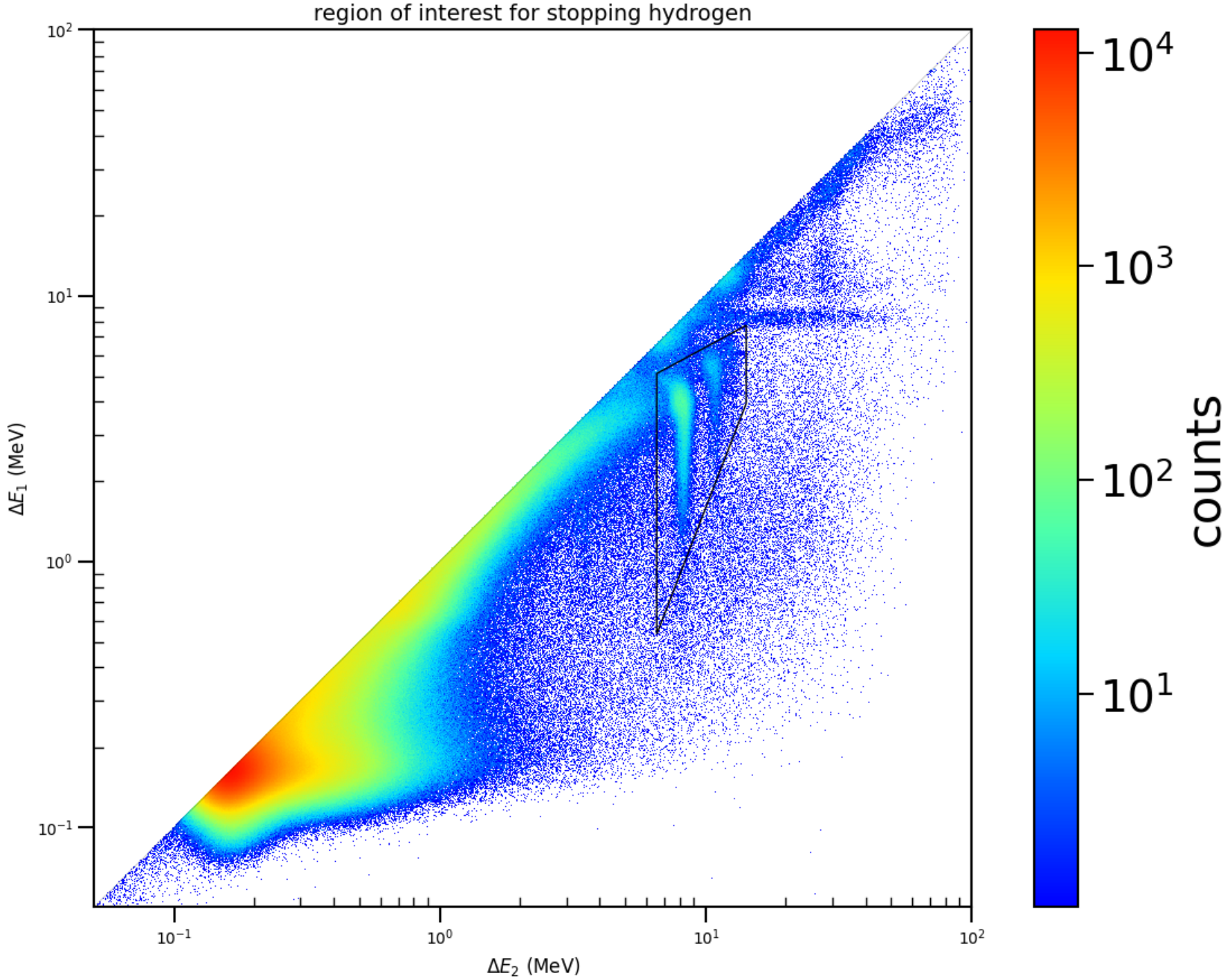

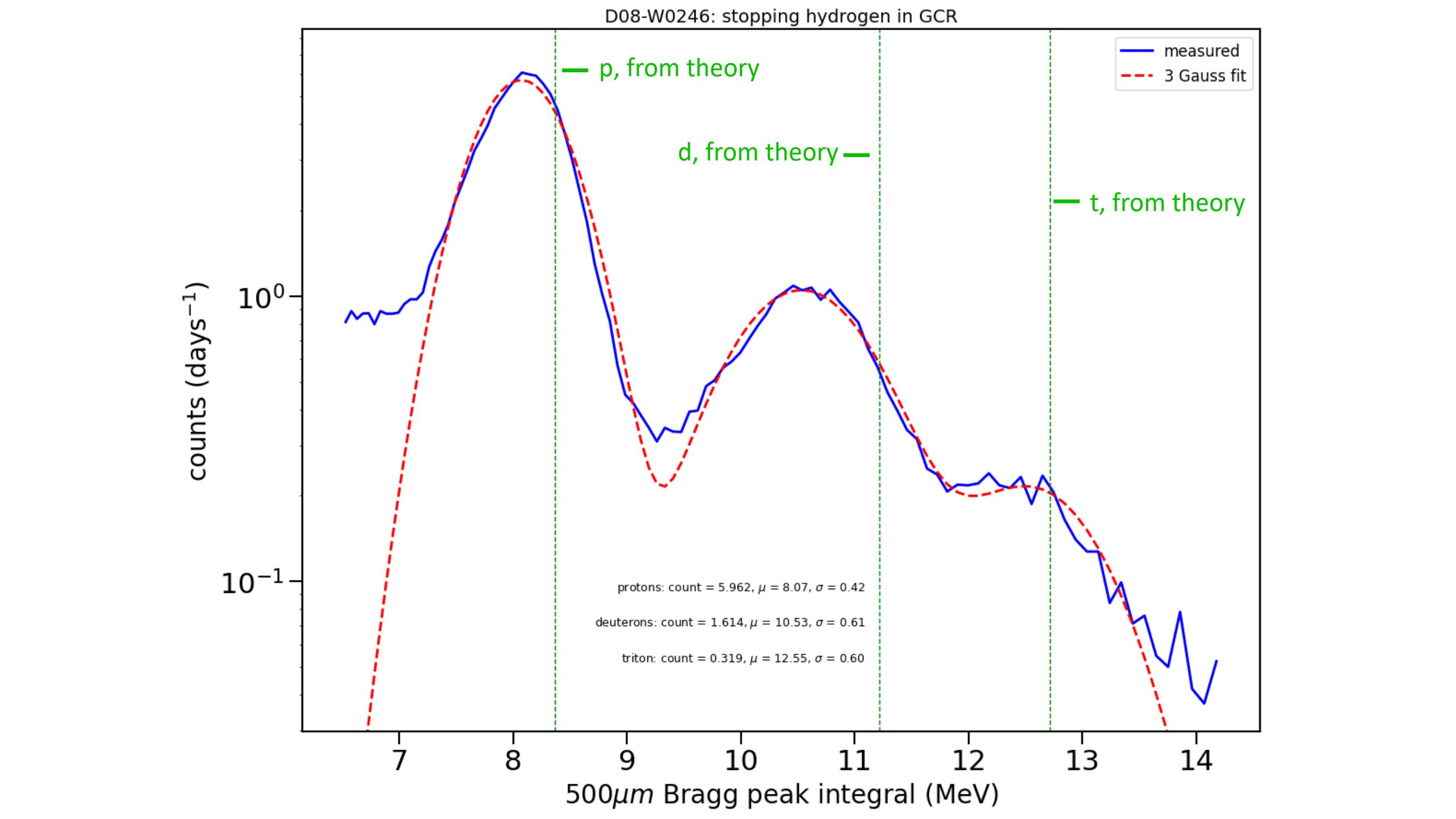
D08-W0246: stopping hydrogen in GCR
measured
3 Gauss fit
p, from theory
d, from theory
t, from theory
protons: count = 5.962, μ = 8.07, σ = 0.42
deuterons: count = 1.614, μ = 10.53, σ = 0.61
triton: count = 0.319, μ = 12.55, σ = 0.60
counts (days⁻¹)
10⁰
10⁻¹
7
8
9
10
11
12
13
14
500μm Bragg peak integral (MeV)

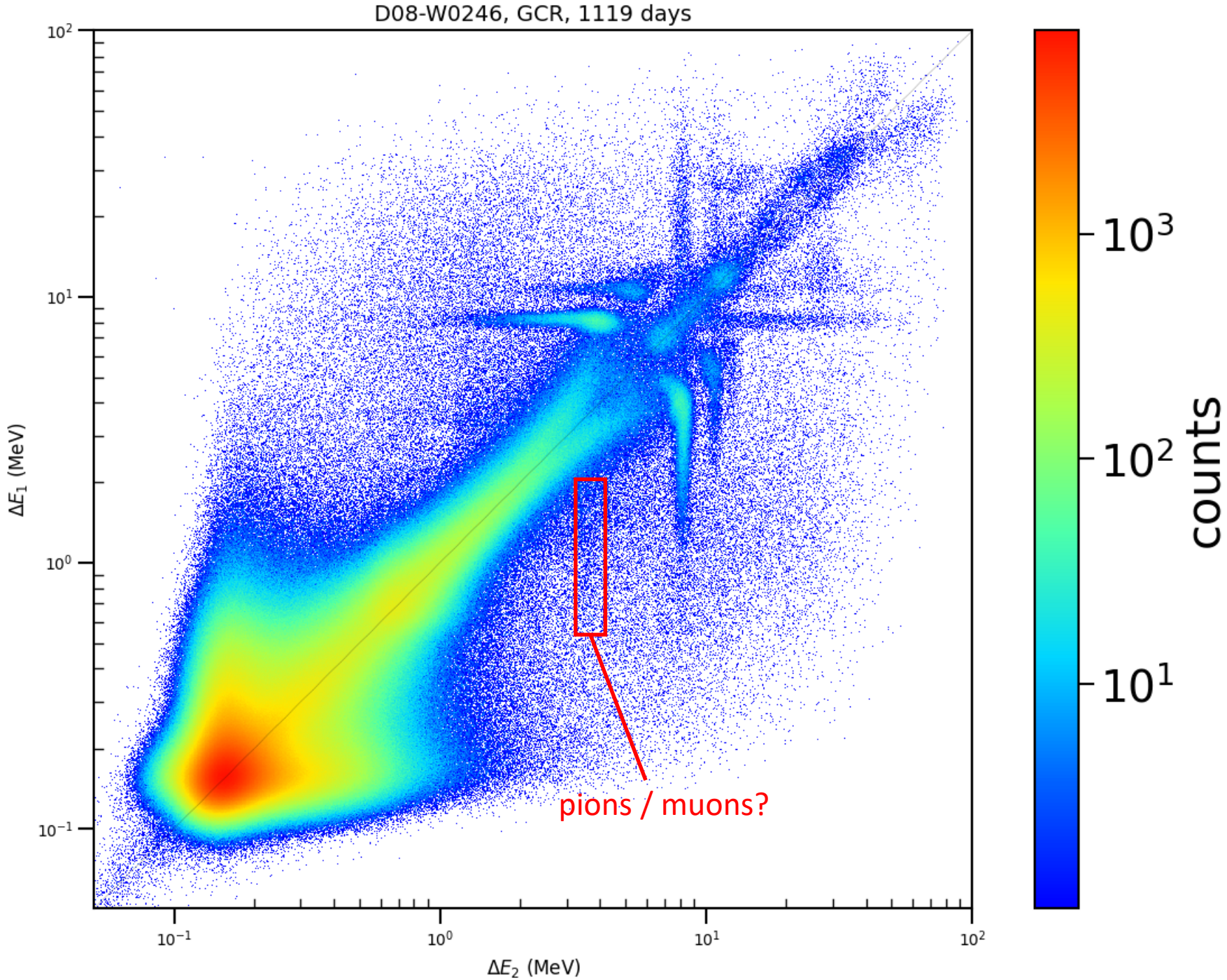
D08-W0246, GCR, 1119 days
10^2
10^1
10^0
10^{-1}
ΔE_1 (MeV)
10^{-1}
10^0
10^1
10^2
ΔE_2 (MeV)
pions / muons?
10^3
10^2
10^1
counts

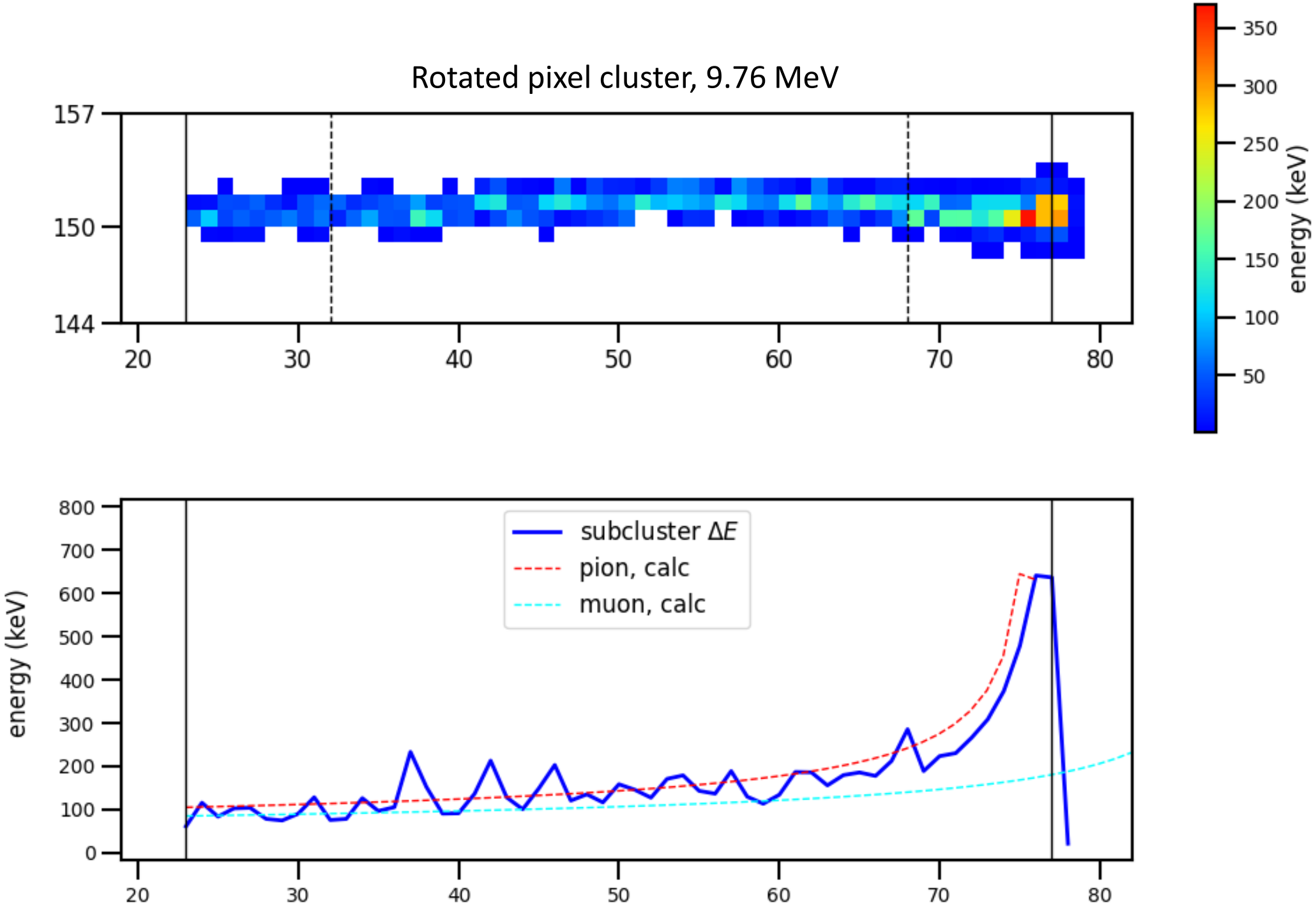
Rotated pixel cluster, 9.76 MeV
157
150
144
20
30
40
50
60
70
80
350
300
250
200
150
100
50
energy (keV)
800
700
600
500
400
300
200
100
0
energy (keV)
subcluster ΔE
pion, calc
muon, calc

References

- ‘Kinetic energy reconstruction with a single layer particle telescope,’ Kroupa *et al*., Applied Physics Letters 112, 134103 (2018)
- ‘Light ion isotope identification in space using pixel detector based single layer telescope,’ Kroupa *et al*., Applied Physics Letters 113, 174101, (2018)

Backup slides

Mean Quality Factor

Region	D08-W0246	E04-W0246	F08-W0246	G05-W0246	I06-W0246	L05-W0246	E04-W0281
GCR	1.89	1.85	1.74	2.73	1.71	1.95	1.71
SAA	1.28	1.37	1.34	1.28	1.40	1.33	1.49
Polar	2.47	2.50	1.96	3.84	2.12	3.16	2.21
All	1.59	1.80	1.64	1.72	1.72	1.78	1.87

Table 1: Table of per region ICRP60 average quality factors.

Northward SAA transit

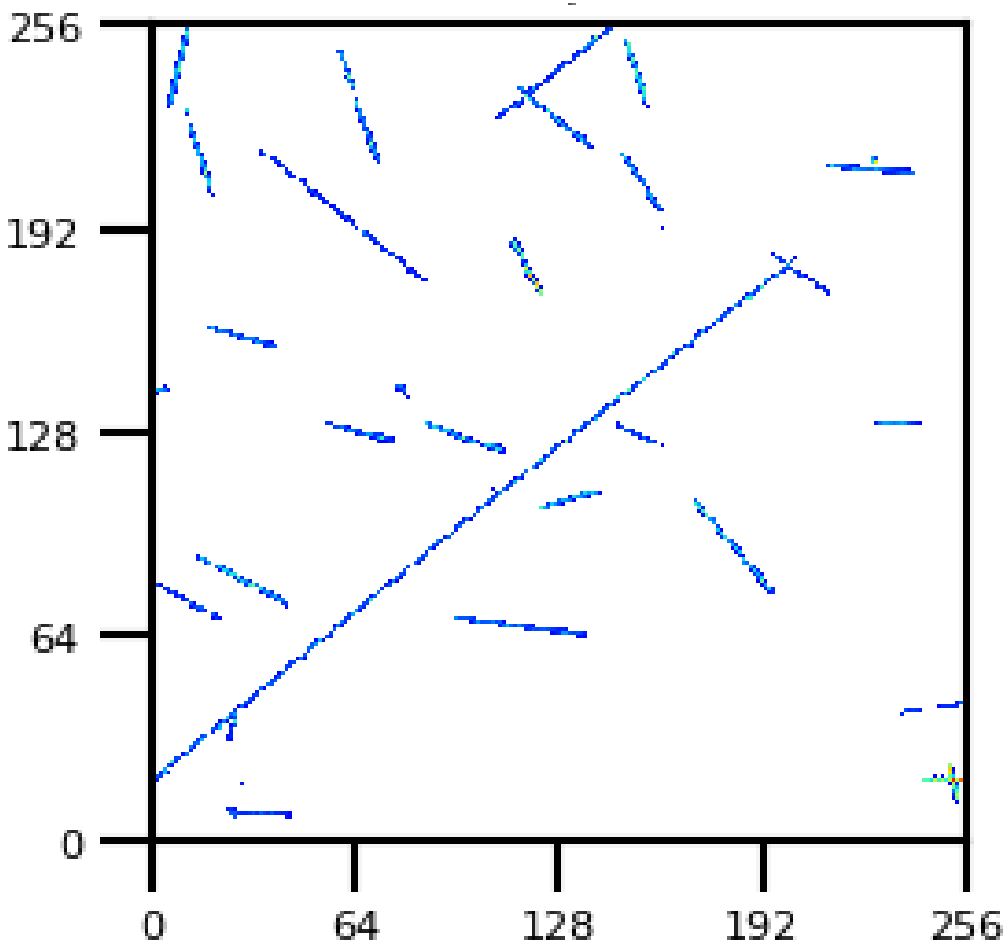

0.129 seconds, 2.3 % occupancy, 31 hits,
0.043 µGy (19.99 µGy / min)

Southward SAA transit

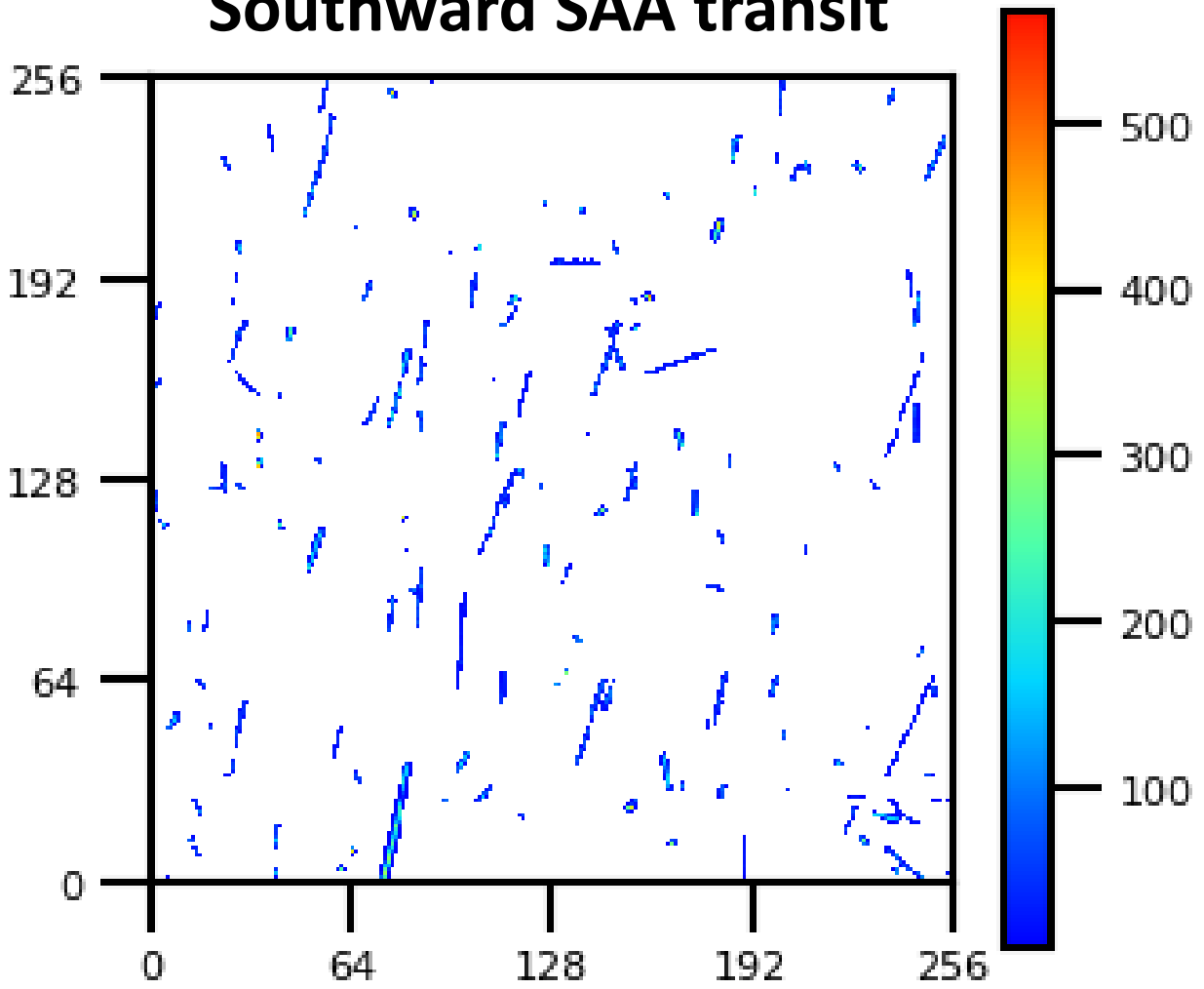

4 seconds, 3.1 % occupancy, 131 hits,
0.066 µGy (0.991 µGy / min)

Detector L05-W0246, located in Node 1

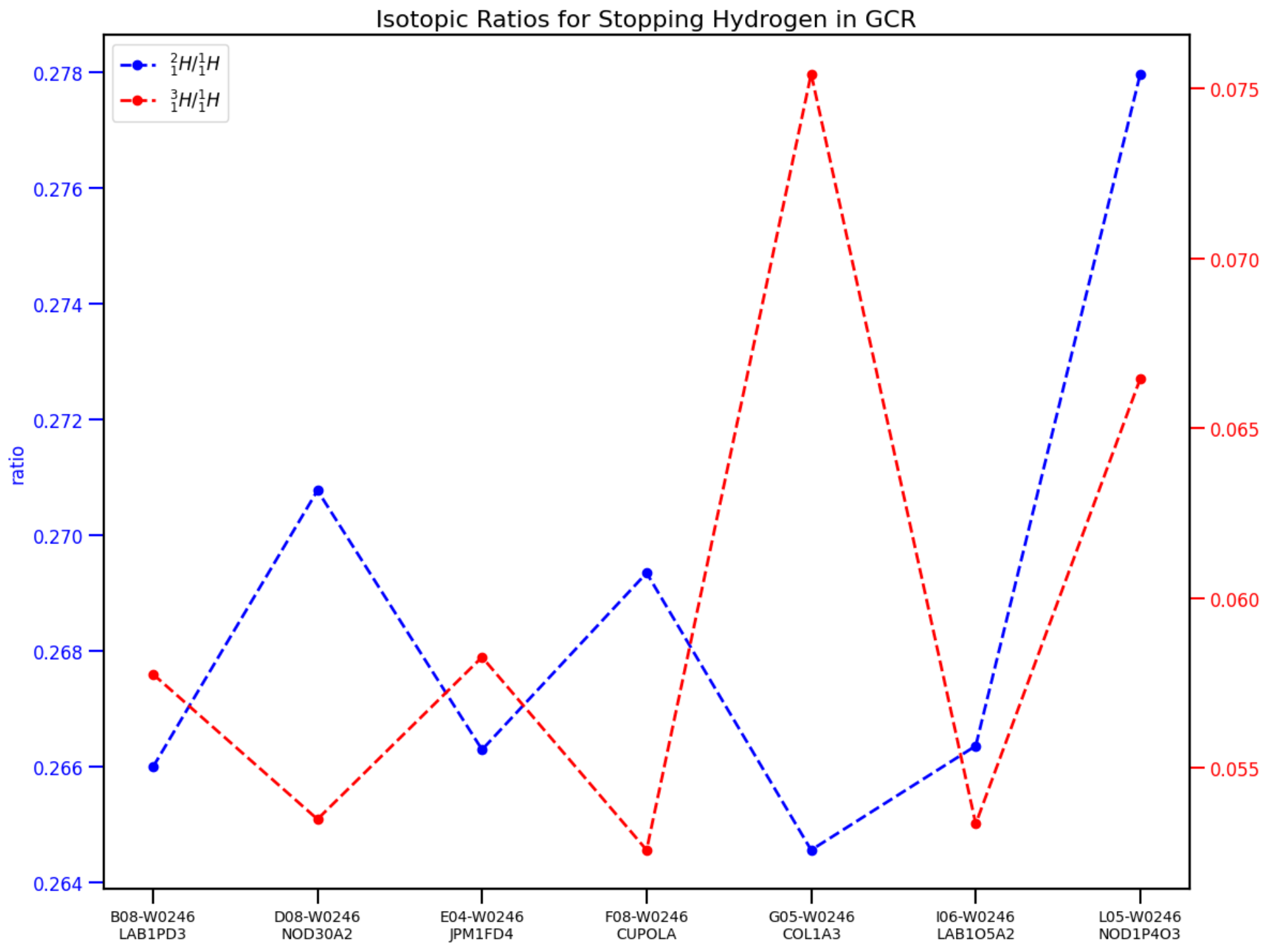
Isotopic Ratios for Stopping Hydrogen in GCR
$^{2}_{1}H/^{1}_{1}H$
$^{3}_{1}H/^{1}_{1}H$
ratio
0.278
0.276
0.274
0.272
0.270
0.268
0.266
0.264
0.075
0.070
0.065
0.060
0.055
B08-W0246
LAB1PD3
D08-W0246
NOD30A2
E04-W0246
JPM1FD4
F08-W0246
CUPOLA
G05-W0246
COL1A3
I06-W0246
LAB1O5A2
L05-W0246
NOD1P4O3

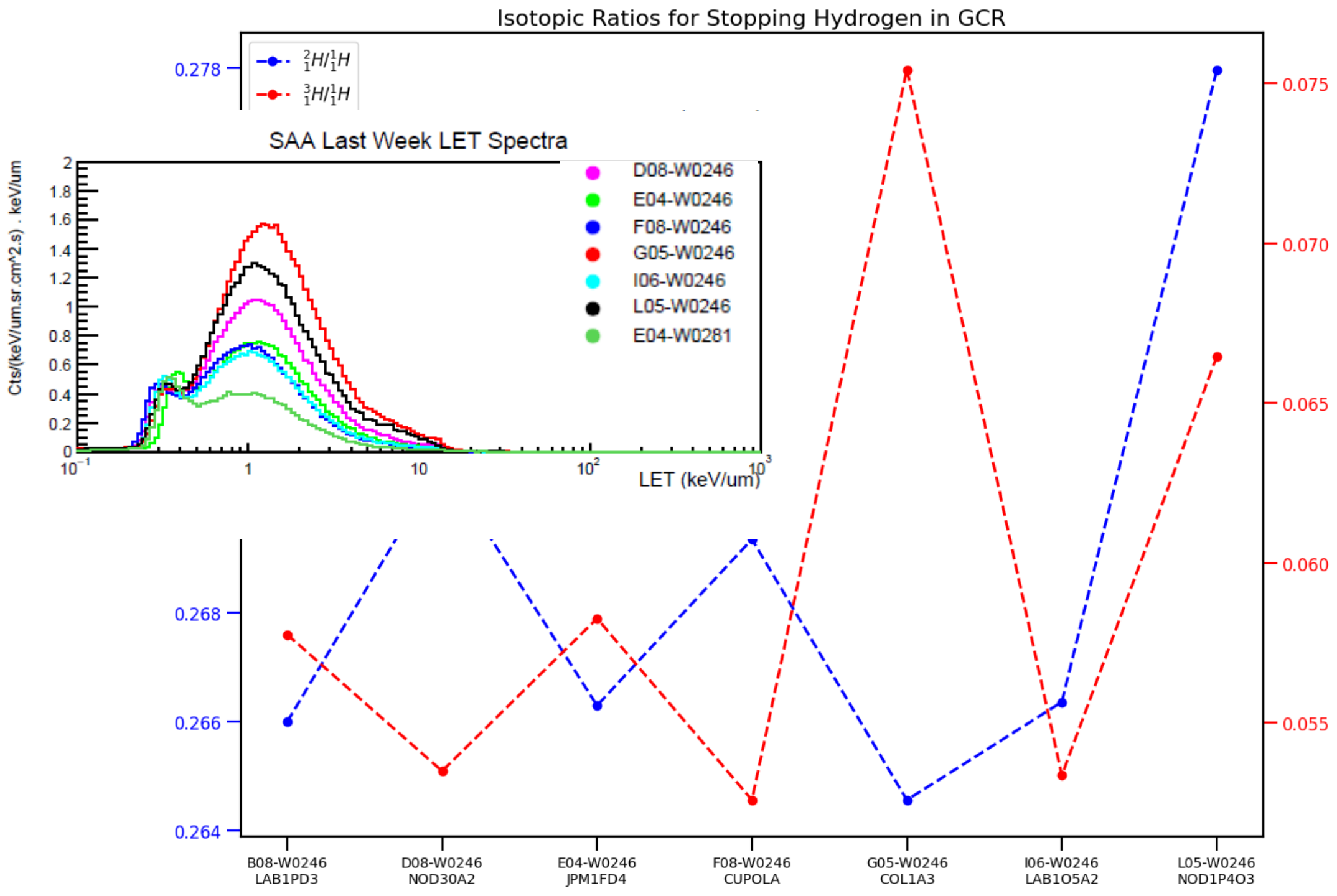
Isotopic Ratios for Stopping Hydrogen in GCR
$^{2}_{1}H/^{1}_{1}H$
$^{3}_{1}H/^{1}_{1}H$
0.278
0.268
0.266
0.264
0.075
0.070
0.065
0.060
0.055
B08-W0246
LAB1PD3
D08-W0246
NOD30A2
E04-W0246
JPM1FD4
F08-W0246
CUPOLA
G05-W0246
COL1A3
I06-W0246
LAB1O5A2
L05-W0246
NOD1P4O3
SAA Last Week LET Spectra
Cts/(keV/um.sr.cm^2.s) . keV/um
LET (keV/um)
D08-W0246
E04-W0246
F08-W0246
G05-W0246
I06-W0246
L05-W0246
E04-W0281

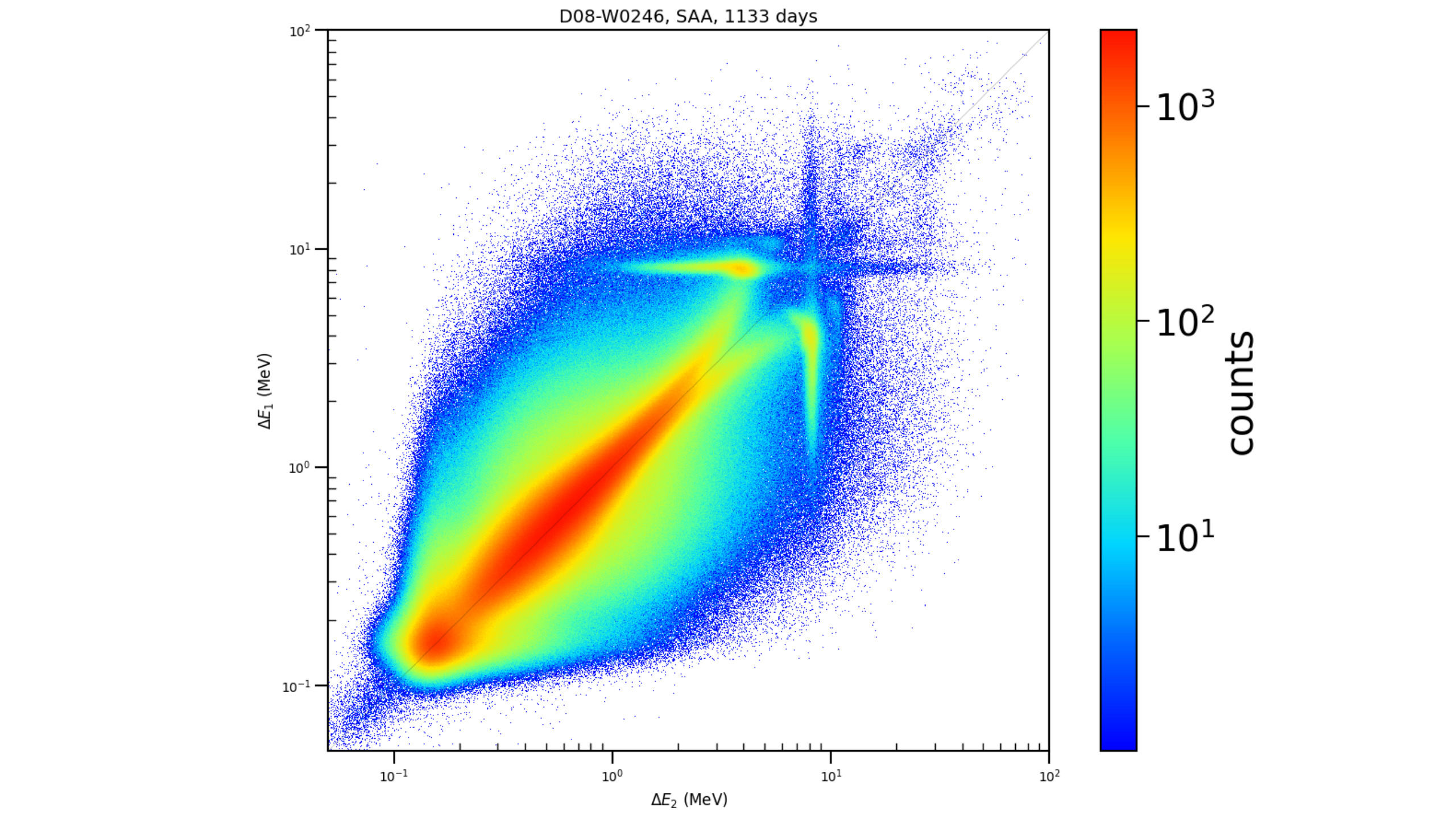
D08-W0246, SAA, 1133 days
10^2
10^1
10^0
10^{-1}
ΔE_1 (MeV)
10^{-1}
10^0
10^1
10^2
ΔE_2 (MeV)
10^3
10^2
10^1
counts

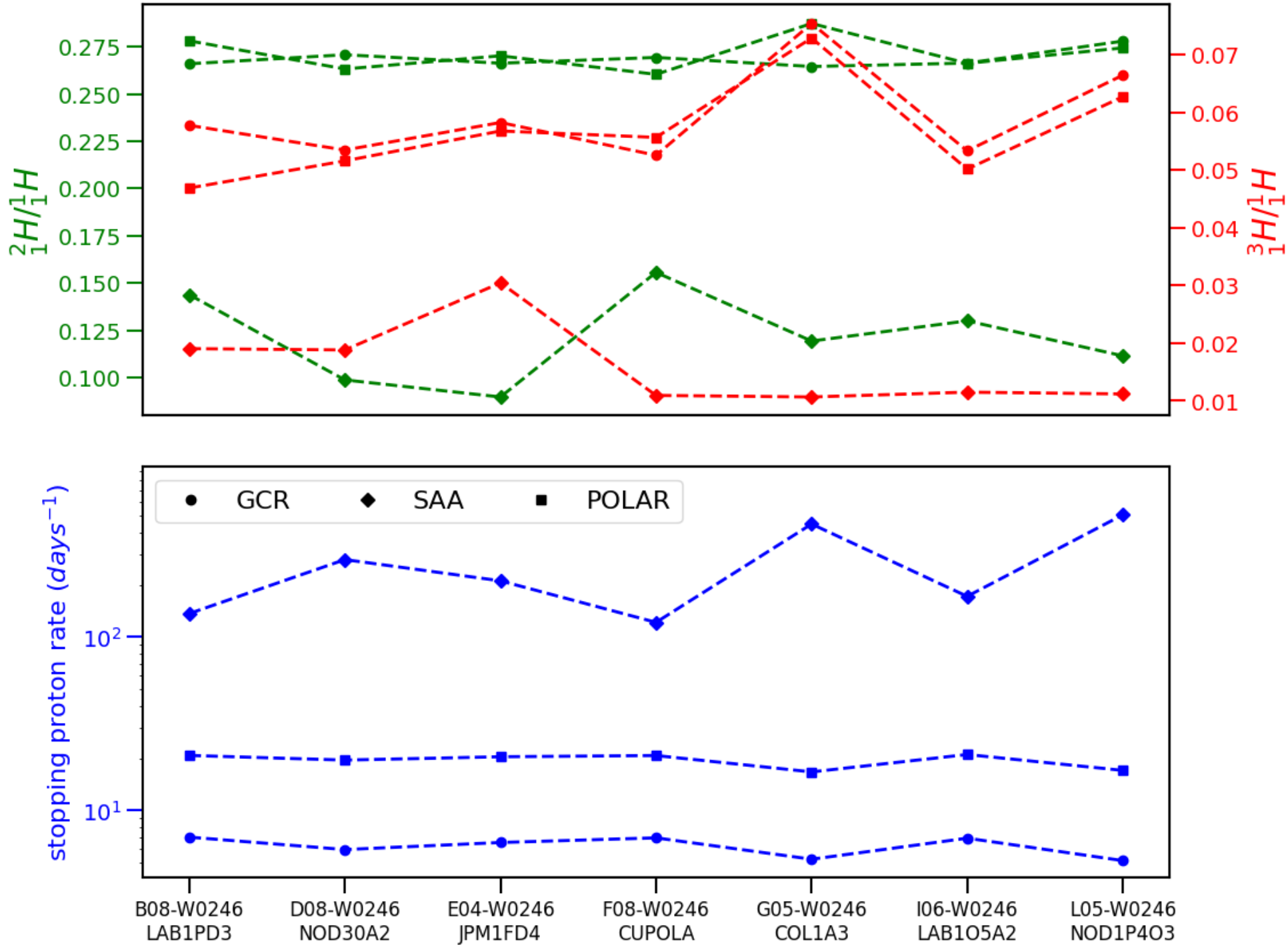
0.275
0.250
0.225
0.200
0.175
0.150
0.125
0.100
$^{2}_{1}H/^{1}_{1}H$
0.07
0.06
0.05
0.04
0.03
0.02
0.01
$^{3}_{1}H/^{1}_{1}H$
GCR
SAA
POLAR
stopping proton rate ($days^{-1}$)
10^{2}
10^{1}
B08-W0246
LAB1PD3
D08-W0246
NOD30A2
E04-W0246
JPM1FD4
F08-W0246
CUPOLA
G05-W0246
COL1A3
I06-W0246
LAB1O5A2
L05-W0246
NOD1P4O3

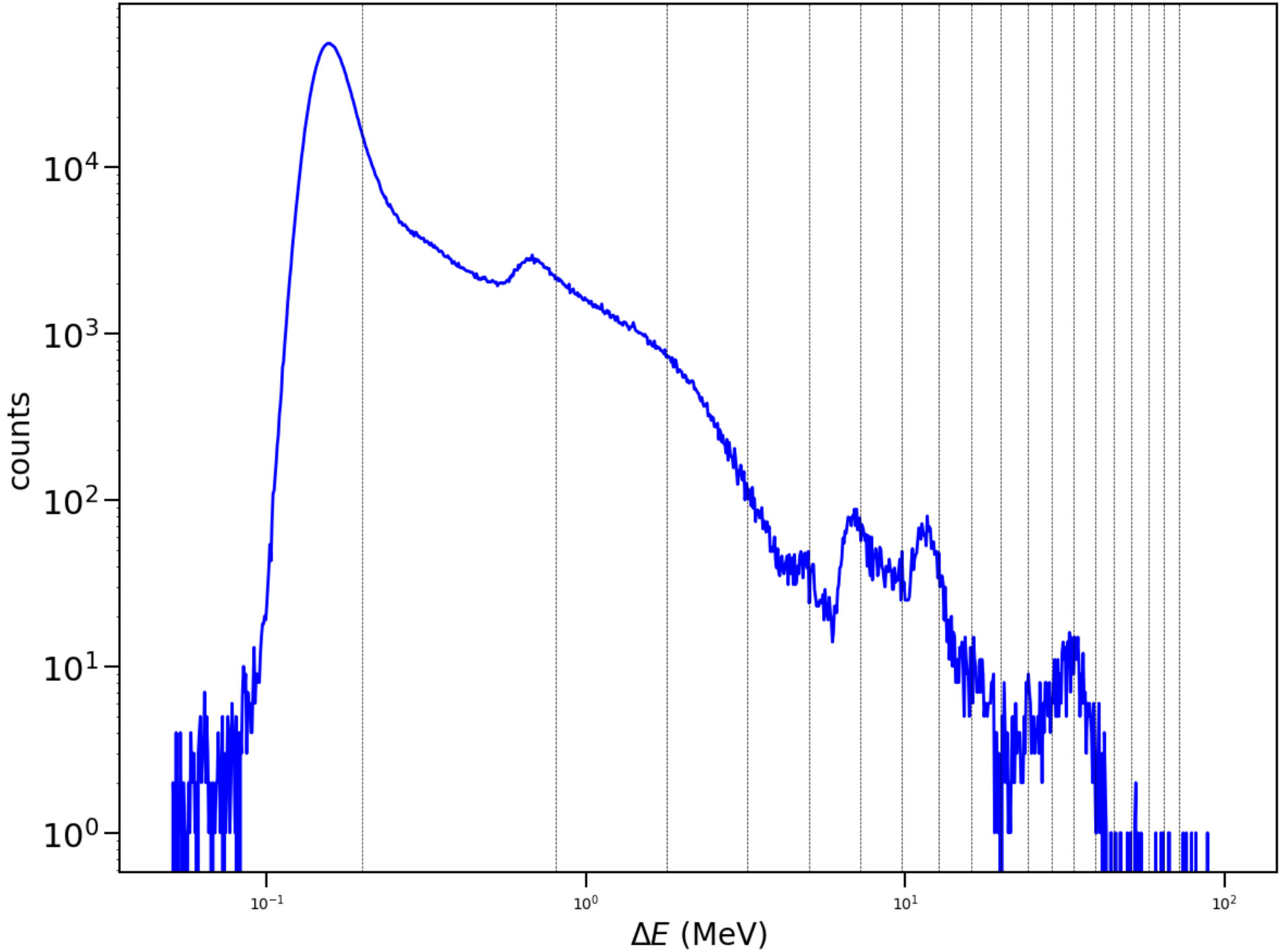
counts
10^4
10^3
10^2
10^1
10^0
10^{-1}
10^0
10^1
10^2
ΔE (MeV)

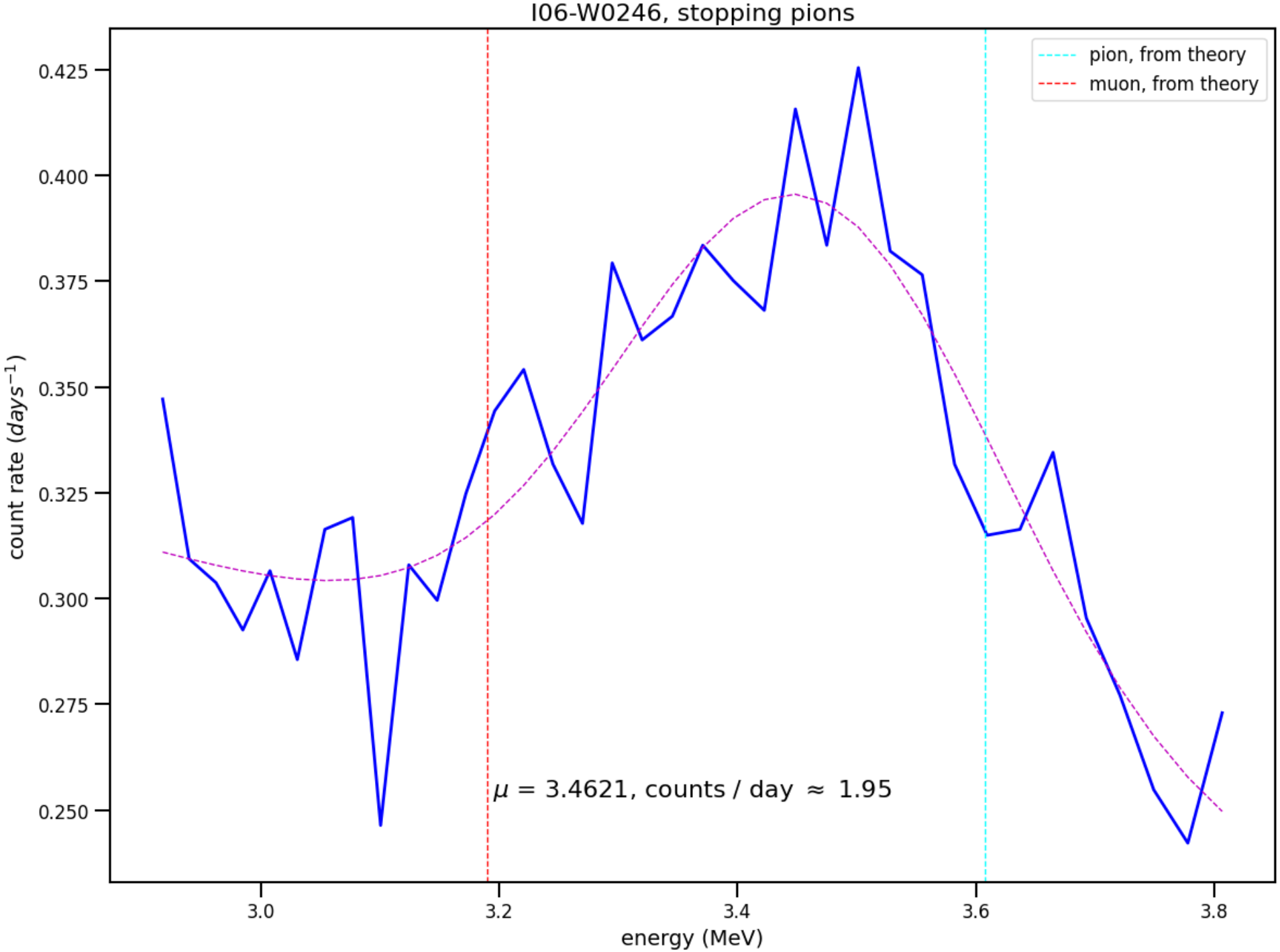
I06-W0246, stopping pions
pion, from theory
muon, from theory
0.425
0.400
0.375
0.350
0.325
0.300
0.275
0.250
count rate ($days^{-1}$)
μ = 3.4621, counts / day $\approx$ 1.95
3.0
3.2
3.4
3.6
3.8
energy (MeV)